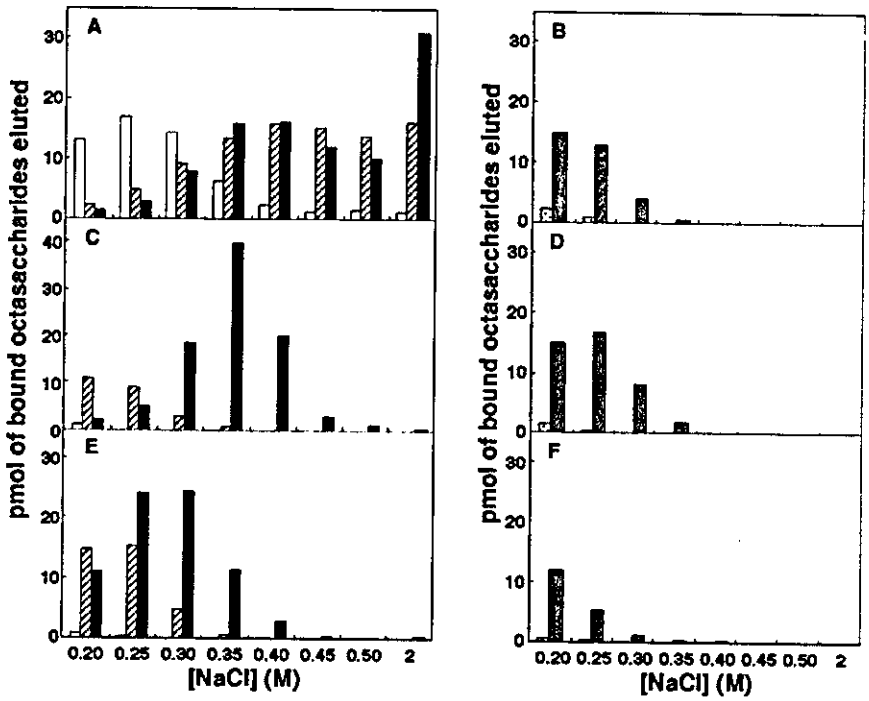

FIG. 4. **Affinity profiles of 2-*O*-sulfated or 6-*O*-sulfated octasaccharides for various growth and differentiation factors.** 100 pmol of octasaccharide was applied to GF affinity columns as described under "Experimental Procedures." After a wash with binding buffer, bound oligosaccharides were eluted with increasingly higher concentrations of NaCl. 2S-1 (*open bars*), 2S-2 (*striped bars*), and 2S-3 (*closed bars*) were subjected to FGF-2 (*A*), FGF-18 (*C*), and HGF (*E*) affinity chromatography. 6S-2 (*dotted bar*) and 6S-3 (*gray bar*) were subjected to FGF-10 (*B*), FGF-18 (*D*), and HGF (*F*) affinity chromatography. Each of the bars indicates the amount of eluted octasaccharide.

one, two, or three 6-*O*-sulfate groups (6S-1, 6S-2, and 6S-3). To the FGF-2-conjugated column, 57% of 2S-1 and more than 90% of 2S-2 and 2S-3 applied were bound. The majority of the bound 2S-1 was released by 0.35 M NaCl, but a complete release of 2S-2 and 2S-3 was attained with 2.0 M NaCl (Fig. 4*A*). These results indicate that the presence of only 1 unit of HexA($2SO_4$)-GlcNSO_3 is sufficient to retain the octasaccharides on FGF-2, and that the affinity of octasaccharides containing 2 or 3 units of HexA($2SO_4$)-GlcNSO_3 to FGF-2 is much higher than that of the other growth factors examined. To the FGF-10-conjugated column, 32% of 6S-3 was bound but neither 6S-2 nor 6S-1 was bound (Fig. 4*B*). These results suggest that 3 units of HexA-Glc$NSO_3(6SO_4)$ are required for the binding of 6-*O*-sulfated Octa-I to FGF-10. Because 48% of the bound 6S-3 was released by 0.25 M NaCl, the interaction of FGF-10 with 6-*O*-sulfated octasaccharides should be relatively weak. As observed in Fig. 3, FGF-18 and HGF showed affinity to both 2-*O*-sulfate and 6-*O*-sulfate, and the affinity to 2-*O*-sulfate seemed to be higher than to 6-*O*-sulfate. These results were confirmed by the binding experiments using different sulfated Octa-I molecules (Fig. 4). To the FGF-18-conjugated column, 90% of 2S-3, 42% of 6S-3, and 23% of 2S-2 were bound, but 6S-2, 6S-1, and 2S-1 were not bound. Quantitative elution of the bound 2S-3 and 6S-3 was achieved with 0.4 and 0.3 M, respectively, of NaCl (Fig. 4, *C* and *D*). Nearly the same results were obtained for the HGF-conjugated column (Fig. 4, *E* and *F*); 75% of 2S-3, 35% of 2S-2, and 19% of 6S-3 were bound, but 2S-1, 6S-2, and 6S-1 were not bound. Quantitative elution of the bound 2S-3 and 6S-3 was achieved with 0.35 and 0.25 M, respectively, of NaCl. However, a clear difference between FGF-18 and HGF was observed in the affinity to 6S-3; the affinity of HGF to 6S-3 was much lower than that of not only FGF-18 to 6S-3 but also HGF to 2S-2. These results indicate that FGF-18 and HGF require at least 2 units of HexA($2SO_4$)-GlcNSO_3 or 3 units of HexA-Glc$NSO_3(6SO_4)$ for the binding of the octasaccharides.

Analysis of the Interactions of $VEGF_{165}$ and BMP-6 with Modified Heparins Using Surface Plasmon Resonance Biosensor—As observed above, $VEGF_{165}$, BMP-6, and FGF-8 were able to bind heparin but did not bind Octa-II. To examine how 2-*O*-sulfate and 6-*O*-sulfate in heparin contributed to the binding to $VEGF_{165}$, BMP-6, and FGF-8, we determined the dissociation constant (K_D) between one of these HBGFs and intact 2-*O*-desulfated (2ODS) or 6-*O*-desulfated (6ODS) heparin. K_D values were determined by surface plasmon resonance (SPR) biosensor. As shown in Table II, 2-*O*-sulfate groups were completely removed from 2ODS-heparin, whereas a few 6-*O*-sulfate groups (up to 1.8%) remained in 6ODS-heparin. The major disaccharide components of heparin, 2ODS-heparin, and 6ODS-heparin were thus thought to be HexA($2SO_4$)-Glc$NSO_3(6SO_4)$, HexA-Glc$NSO_3(6SO_4)$, and HexA($2SO_4$)-GlcNSO_3, respectively. As positive controls, K_D values were also determined for FGF-2 and HGF. The K_D value observed in the system of FGF-2/heparin, FGF-2/2ODS-heparin, and FGF-2/6ODS-heparin was 23, 340, and 23 nM, respectively (Fig. 5, *A–C*, and Table III). Because the K_D for FGF-2/6ODS-heparin was the same as the K_D for FGF-2/heparin, the presence of 6-*O*-sulfated groups on GlcNSO_3 residues in heparin appeared to have no effect on the interaction between FGF-2 and heparin. In contrast, the K_D for FGF-2/2ODS-heparin was 15-fold that for FGF-2/heparin. In the case of HGF, the measured K_D for HGF/heparin, HGF/2ODS-heparin, and HGF/6ODS-heparin was 12, 86, and 58 nM, respectively (Fig. 5, *D–F*, and Table III). Both the K_D for HGF/2ODS-heparin and the K_D for HGF/6ODS-heparin were higher than the K_D values for HGF/heparin. These observed K_D values for the interactions of FGF-2 or HGF with the modified heparins are consistent with the results obtained from the octasaccharide library, and confirm the importance of 2-*O*-sulfate in the binding of FGF-2 and the importance of both 2-*O*- and 6-*O*-sulfate in the binding of HGF. Thus, the K_D values obtained by SPR biosensor using biotinylated glycosaminoglycans seem accurate enough to be compared quantitatively. Under the same conditions used for the interaction of FGF-2 and HGF, we determined K_D values for the interaction between $VEGF_{165}$ or BMP-6 and heparin or the modified ones. The measured K_D for $VEGF_{165}$/heparin, $VEGF_{165}$/2ODS-heparin, and $VEGF_{165}$/6ODS-heparin was 165, 524, and 592 nM, respectively (Fig. 5, *G–I*, and Table III). Both the K_D for $VEGF_{165}$/2ODS-heparin and the K_D for $VEGF_{165}$/6ODS-heparin were 3-fold the K_D values for $VEGF_{165}$/heparin. The measured K_D values for BMP-6/heparin, BMP-6/2ODS-heparin, and BMP-6/6ODS-heparin was 6.3, 11, and 15 nM, respectively (Fig. 5, *J–L*, and Table III), which indicate the

TABLE II
Disaccharide compositions of heparin and modified heparins

Disaccharide component	Heparin	2ODS-heparin	6ODS-heparin
	%	%	%
HexA-GlcNAc	5	6	7
HexA-GlcNS	1	12	10
HexA-GlcNAc(6S)	2	5	ND[a]
HexA(2S)-GlcNS	14	ND	75
HexA-GlcNS(6S)	7	77	6
HexA(2S)-GlcNS(6S)	71	ND	2

[a] ND, not detected.

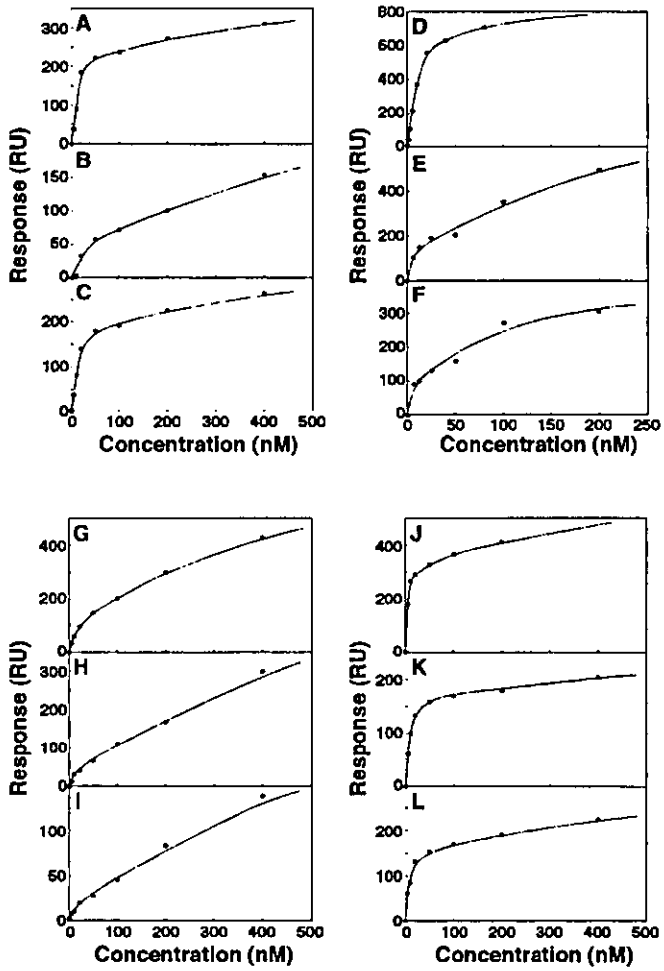

FIG. 5. **The response in steady state level plotted against the concentration of FGF-2, HGF, $VEGF_{165}$, and BMP-6.** Various concentrations of FGF-2 (*A–C*), HGF (*D–F*), $VEGF_{165}$ (*G–I*), and BMP-6 (*J–L*) were injected over the sensor tip-immobilized heparin (*A, D, G,* and *J*), 2ODS-heparin (*B, E, H,* and *K*), and 6ODS-heparin (*C, F, I,* and *L*). The response in the steady state was plotted against the concentration of each GF. The dissociation constant for the interaction was evaluated with these curves using BIA evaluation software.

TABLE III
Equilibrium dissociation constant for the interactions of FGF-2, HGF, $VEGF_{165}$, and BMP-6 with various chemically modified heparins
The K_D (nM) value was measured from Fig. 5.

Immobilized GAG	FGF-2	HGF	$VEGF_{165}$	BMP-6
Heparin	23	12	165	6.3
2ODS-heparin	340	86	524	11
6ODS-heparin	23	58	592	15

extremely high affinity of BMP-6 to heparin or the modified heparins. Even so, both the K_D for BMP-6/2ODS-heparin and the K_D for BMP-6/6ODS-heparin were 2- or 3-fold the K_D values for BMP-6/heparin. These results suggest that both 2-*O*-sulfate groups on HexA residues and 6-*O*-sulfate groups on $GlcNSO_3$ residues contained in heparin/HS are equally required for the interactions with $VEGF_{165}$ and BMP-6.

Because FGF-8 was bound nonspecifically to the sensor chips, the K_D values for FGF-8/modified heparins could not be determined. It should be of note here that no interactions between these growth factors and chondroitin 4-sulfate have been recognized (data not shown).

FGF-releasing Activity of Octasaccharide Library—As shown above, FGF-2 and FGF-10 bound the octasaccharides typically different from each other in that FGF-2 required 2-*O*-sulfate but FGF-10 needed 6-*O*-sulfate. Therefore, we examined whether the addition of 2-*O*-sulfated Octa-I and 6-*O*-sulfated Octa-I could release FGF-2 and FGF-10, respectively, from their complexes with pig aorta HS, which has the affinity for both FGF-2 and FGF-10 and is thought to represent natural HS in normal tissues. Streptavidin-coated ELISA plates were coated with the biotinylated HS. Digoxigenin-labeled FGF-2 or FGF-10 was then added to form complexes with the HS on plates. The incubation with various octasaccharides at different concentrations added to the plates released the digoxigenin-labeled FGF from the complexes, which was assessed by quantitating the labeled FGF left on the plates after several washes as described under "Experimental Procedures." The addition of 1 nmol/ml 6S-3 and 2S-3 released 29 and 8% of bound FGF-10, respectively (Fig. 6*A*), which corresponded to the releasing activity observed by the addition of 0.3 and 0.03 nmol/ml Octa-II, respectively (Fig. 6*B*), suggesting that 6S-3 is 10-fold more active in releasing FGF-10 than 2S-3. The addition of 1 nmol/ml Octa-II released 45% of bound FGF-10. Other *O*-sulfated Octa-I have none or only a slight effect on the releasing. In the case of the FGF-2 binding to the HS, the addition of 0.2 nmol/ml 2S-2, 2S-3, and Octa-II had almost the same releasing activity (57–61%), and that of 0.2 nmol/ml 2S-1 and 6S-3 released 26 and 11% of bound FGF-2, respectively (Fig. 6*C*), which corresponded to the releasing when 0.05 and 0.02 nmol/ml Octa-II were added, respectively (Fig. 6*D*). 2S-1 still showed 25% of the Octa-II activity although it had only one *O*-sulfate, but 6S-3 showed less than 10% of the Octa-II activity even though it had three *O*-sulfate residues. The observed differences of octasaccharide library in the releasing activity are good reflections of the differences in the binding specificity and activity of octasaccharide library to FGF-2 and FGF-10, which were described above.

DISCUSSION

We demonstrated that octasaccharide libraries composed of well defined sulfated octasaccharides generated by recombinant HS-*O*-sulfotransferases were useful for characterizing the binding structure for HBGFs. For FGF-2, FGF-4, FGF-7, FGF-8, FGF-10, FGF-18, HGF, BMP-6, and $VEGF_{165}$, we analyzed systematically the binding structures present in heparin/heparan sulfate, including the octasaccharide library. Based upon differences in affinity, these growth factors could be classified roughly into five groups. Group 1 had the affinity for 2-*O*-sulfated but not 6-*O*-sulfated octasaccharides (FGF-2). Group 2 had the affinity for 6-*O*-sulfated but not 2-*O*-sulfated octasaccharides (FGF-10). Group 3 had the affinity for both 2-*O*-sulfated and 6-*O*-sulfated octasaccharides but preferred 2-*O*-sulfated ones (FGF-18 and HGF). Group 4 required both 2-*O*-sulfate and 6-*O*-sulfate in octasaccharides for binding (FGF-4 and FGF-7). Group 5 hardly bound any octasaccharides significantly (FGF-8, BMP-6, and VEGF) (Fig. 7). The results indicate that the structural domain in heparin/heparan sulfate exhibiting affinity to each HBGF could be differentiated in terms of chain size, position to which the sulfate is attached,

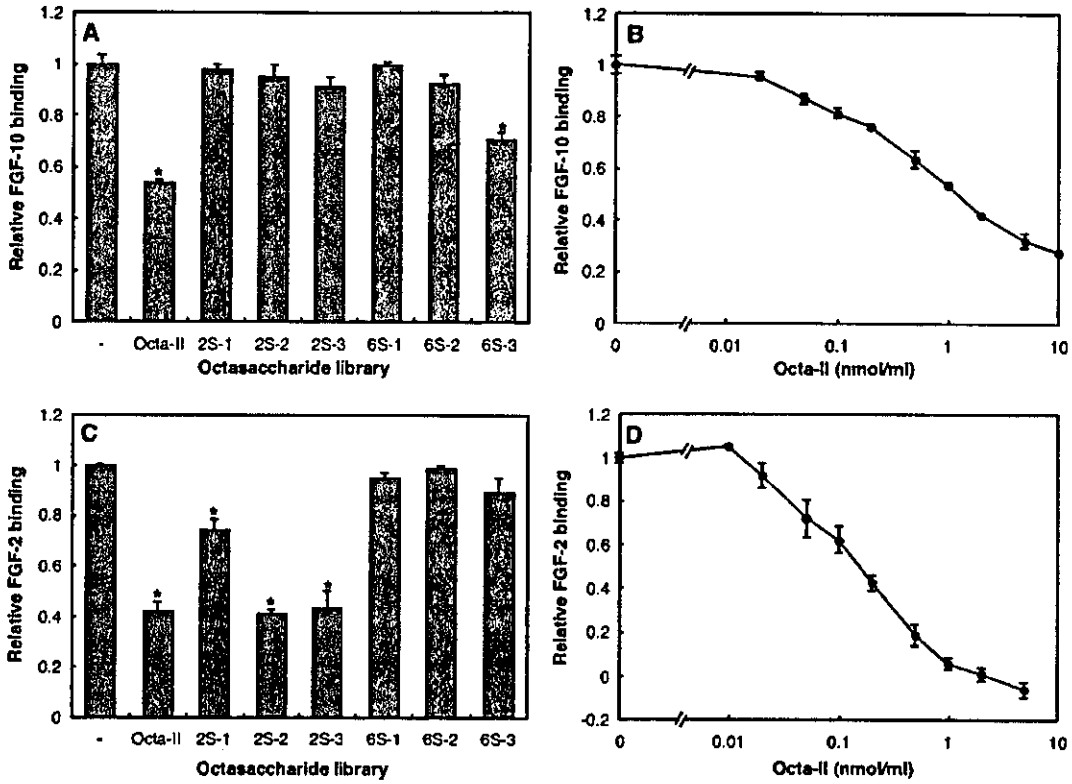

FIG. 6. **FGF-10 and FGF-2 releasing activity of octasaccharide library from the complex with HS.** Releasing activity was detected by ELISA as described under "Experimental Procedures." Digoxigenin-labeled FGF-10 (*A* and *B*) or FGF-2 (*C* and *D*) was added into wells coated with HS (0.1 nmol as hexuronic acid). After 1 h, unbound digoxigenin-labeled FGF was removed. Then 1 (*A*) and 0.2 nmol/ml (*C*) of octasaccharide library and Octa-II at various concentrations (*B* and *D*) were added. After 1 h, the wells were washed, and then anti-digoxigenin-AP, Fab fragments were added to yield color. Nonspecific binding was determined in the absence of FGFs. The experiments were independently repeated three times. The *columns* show mean values ± S.D. Statistical analyses were performed using Student's *t* test. Significance when compared with control was shown by the *asterisk* representing $p < 0.05$.

and the number and probably distribution of sulfate groups within the binding domain.

We also demonstrated relevance of the use of an octasaccharide library consisting of defined sulfated octasaccharides for characterizing the binding structures for HBGFs by their releasing activities of HBGFs from the complexes of HS and HBGFs. The affinity analyses using octasaccharide library revealed unique and almost opposite structural requirements for the bindings of FGF-10 and FGF-2. Therefore, we examined whether the addition of octasaccharides having the affinity to FGF-10 and FGF-2 could release FGF-10 and FGF-2, respectively, from their complexes with aorta HS. As expected from the affinity analyses, octasaccharides with the high affinity to FGF-10 or FGF-2 released specifically the respective FGF from their complexes with HS, and in addition, octasaccharides with the higher affinity gave the higher releasing activity (Fig. 6). These results suggest that the interactions of HS with certain HBGFs involved regions of the HS with specific sulfation patterns, and the exogenous addition or the endogenous generation of such regions as oligosaccharides may affect the bindings of HBGFs to HS and also to HBGF receptors. In the case of FGF, because HS is also known to bind to the growth factor receptors, the supply of HS oligosaccharides, whether it is exogenous or endogenous, may have some effect on their signaling. Further investigation remains on functions as the signaling regulators of these oligosaccharides.

Heparin-binding structures of the FGF family have been investigated by x-ray crystallographic analysis and biochemical analysis (36–38). From these studies, several basic amino acid residues were found to exist opposite the 2-*O*-sulfate group in heparin. Our results indicated that some members of the FGF family examined here had affinity to 2-*O*-sulfate, but FGF-10 exhibited little affinity to 2-*O*-sulfate. Instead, FGF-10 had affinity to the 6-*O*-sulfate group. To investigate whether the amino acid residues interacting with 2-*O*-sulfate groups are conserved in FGF-10, the putative heparin-binding region of FGF-10 was aligned with the same regions of other members of the FGF family having affinity to the 2-*O*-sulfate group (Fig. 7). It has been shown that the 2-*O*-sulfate-binding region of FGF-2 consists of Lys-125, Gln-134, Lys-135, and Ala-136 (39), whereas that of FGF-1 is composed of Asn-18, Lys-113, Lys-118, and Gln-127 (40) (see boldface amino acid residues in the partial amino acid sequences of FGF-2 and FGF-1 in Fig. 7). When the glycine boxes, which are commonly found in the FGF family and thought to correspond to motifs for heparin-binding sites, are aligned among FGF-2, FGF-4, FGF-7, FGF-8, FGF-10, and FGF-18, either Gln or Lys residues found in these putative 2-*O*-sulfate-binding sites are conserved in FGF-4, -7, -8, and -18 (see amino acid residues in the *gray boxes* in Fig. 7). However, these residues are not conserved in FGF-10 at all but are substituted for other amino acids. Crystallographic analysis of the FGF-10-heparin oligosaccharide complex will reveal the structure of the heparin-binding domain of FGF-10.

We demonstrated previously that the HGF-bound octasaccharide prepared from bovine liver HS contained 2 units of $IdoUA(2SO_4)$-$GlcNSO_3(6SO_4)$, whereas the HGF-unbound octasaccharide from the same HS contained only 1 unit of $IdoUA(2SO_4)$-$GlcNSO_3(6SO_4)$. On the other hand, Lyon *et al.* (29) reported that 2-*O*-sulfate groups contributed marginally to the interaction between HGF and fibroblast HS. Such an apparent discrepancy may be due partly to the difference in the heparan sulfate used. The present study clearly shows that HGF interacts with both 2-*O*-sulfate and 6-*O*-sulfate, because both the 2-*O*-sulfated octasaccharides containing 2 or 3 units of

Groups	(Necessary *O*-sulfate in octasaccharide)	GF		heparin binding regions of FGFs
				Glycine box
Group 1	(2-*O*-sulfate)	FGF-2	118 L	K R T G Q Y **K** L G S K T G P G **Q K A** I L
Group 2	(6-*O*-sulfate)	FGF-10	180 L	N G K G A P R R G Q K T R R K N T S A H
Group 3	(2-*O*- or 6-*O*-sulfate)	FGF-18	153 F	T **K** K G R P R K G P K T R E N **Q** Q D V H
		HGF		
Group 4	(2-*O*- and 6-*O*-sulfate)	FGF-4	181 L	S **K** N G K T **K** K G N R V S P T M **K** V T H
		FGF-7	167 L	N Q K G I P V R G K K T K K E **Q K** T A H
		(FGF-1)	111 L	K **K** N G S C **K** R G P R T H Y G **Q K A** I L
Group 5		FGF-8	171 F	T R K G R P R K G S K T R Q H **Q** R E V H
		VEGF		
		BMP-6		

FIG. 7. **Summary of *O*-sulfate essential for GF binding and comparison of heparin-binding regions in different FGFs.** The sequence alignment was performed using the ClustalW program (34, 36). All of the FGFs used in this alignment are from human. The sequences of the putative heparin-binding regions of FGFs that are structurally superimposed are shown, where the 2-*O*-sulfate-binding residues are indicated in *boldface*. *Square* shows glycine box, which is thought to correspond to motifs for heparin-binding sites (37).

HexA(2SO_4)-GlcNSO_3 and the 6-*O*-sulfated octasaccharides containing 3 units of HexA-GlcNSO_3(6SO_4) were bound to HGF. The fact that both 2-*O*-sulfate and 6-*O*-sulfate are involved in the interaction between HGF and HS was also supported by the crystallographic analysis of NK1 (a spliced variant of HGF)-heparin complexes. In this system, the 2-*O*-sulfate of HexA makes a hydrogen bond with Arg-73, whereas 6-*O*-sulfate of GlcNSO_3 makes a hydrogen bond with Lys-63 (41). In SPR analysis, the 2-*O*-desulfated heparin and 6-*O*-desulfated heparin prepared by region-selective desulfation dissociated faster from HGF than the native heparin (data not shown), supporting that both 2-*O*-sulfate groups in IdoUA and 6-*O*-sulfate groups in GlcNSO_3 play important roles in maintaining interaction with HGF.

We demonstrated that $VEGF_{165}$ did not bind octasaccharides with both 2-*O*- and 6-*O*-sulfate groups at all but bound the native heparin, indicating that $VEGF_{165}$ requires a longer binding domain than octasaccharide for binding heparin. Both 2-*O*-sulfate groups on HexA residues and 6-*O*-sulfate groups on GlcNSO_3 residues appear to contribute equally to the interaction between $VEGF_{165}$ and heparin, because the K_D value for $VEGF_{165}$/2ODS-heparin was nearly equal to the K_D value for $VEGF_{165}$/6ODS-heparin. Although the K_D value for $VEGF_{165}$/heparin was much larger than that for FGF-2/heparin or HGF/heparin, the interaction between $VEGF_{165}$ and heparin may still have relevance to some physiological processes, because the activity of $VEGF_{165}$ was stimulated *in vitro* by heparin, and mutant mice expressing only $VEGF_{121}$ lacking the heparin-binding domain showed abnormalities of microvascularization. Four spliced variants of VEGF, $VEGF_{145}$, $VEGF_{165}$, $VEGF_{189}$, and $VEGF_{206}$, may thus have important physiological functions through the interaction with HS. It remains to be studied what structures in HS could interact with the spliced variants other than $VEGF_{165}$ and how strong binding activity is.

To our knowledge, the direct interaction between BMPs and heparan sulfate has never been studied. However, there are a number of reports to suggest important roles of the interaction in differentiation and morphogenesis. For example, glypican-3, one of a family of six cell surface heparan sulfate proteoglycans in vertebrates, plays an important role in BMP signaling during limb patterning and skeletal development (42) and renal branching morphogenesis (43). The interaction of Dally, a glypican homolog, and Decapentaplegic, a TGF-β/BMP homolog, in *Drosophila* functions in the gradient formation of Decapentaplegic as a morphogen necessary for the wing and sensory organ formation (44–46). In the present study, we have shown that BMP-6 did not bind any octasaccharide, but by SPR analysis it bound heparin and 2ODS- or 6ODS-heparin with conspicuously high affinity. Chondroitin sulfate and CDSNS-heparin were a very poor ligand (data not shown). Therefore, the interaction with heparan sulfate should be very strong if the *O*-sulfated region is long enough. It is known that inducing activities of some members of the BMP family are tightly restricted to the region around the cells that produce them (47). Therefore, the observed high affinity of BMP-6 in the binding to HS likely reflects a role of HS in trapping the BMP. Because there are a number of the BMP family molecules with different activities (48), the present study raises an interesting question how each of them interacts with HS.

In our study Octa-II, octasaccharide containing three HexA(2SO_4)-GlcNSO_3(6SO_4) units derived from heparinase-digested heparin did not have the affinity enough to bind to FGF-8-conjugated column under the used conditions (Fig. 2). Because heparin was almost retained to this column, we judged FGF-8 needed the longer size for the binding. However, the minimal saccharide domain for the binding of FGF-8b, a spliced variant of FGF-8, has been reported to encompass 5–7 monosaccharide units of heparin (28). The observed discrepancy might have been caused by our usage of FGF-8, which is not a spliced variant, by some alteration in binding properties such as partial denaturation of our FGF-8 or by the difference in the reducing and nonreducing ends of oligosaccharide structures due to the preparation methods between ours (heparinase digestion) and theirs (nitrous acid degradation).

We prepared sulfated octasaccharides using the recombinant HS2ST and HS6ST-1. Up to 3 units of 2-*O*-sulfate could be introduced to the acceptor octasaccharide under the reaction conditions used here. Three units of 2-*O*-sulfate are probably the upper limit of sulfation, because unsaturated uronic acid at the nonreducing end of Octa-I could not be sulfated. When 60% of the acceptor substrate was converted to the 2-*O*-sulfated products, the octasaccharide having 1–3 units of 2-*O*-sulfate

was obtained at a ratio of 1.0:0.40:0.15. The one having 1 unit of 2-*O*-sulfate was a major product at the beginning of the reaction (Fig. 1, *insets*). It is thus unlikely that the sulfated octasaccharides behave better as an acceptor for HS2ST than the nonsulfated octasaccharide. As observed in the products of HS6ST-1, 6-*O*-sulfated Octa-I also separated into three major peaks; the octasaccharides with 1 unit of 6-*O*-sulfate were obtained in the highest yield even at the end of the reaction. HS6ST-1 appears to prefer nonsulfated octasaccharide as well. A small peak was observed after 6S-3 in the Mono Q chromatography. This peak may be an octasaccharide with 4 units of 6-*O*-sulfate groups, although the disaccharide composition of this peak has yet to be determined. It is of interest to examine the order and extent of 6-*O*-sulfation with HS6ST-1.

There are now a number of studies to demonstrate that HS is important to activate the growth factor binding to its receptor via the complex formation among them (5, 9), and longer HS oligosaccharides such as decasaccharides are involved in those interactions (25). Therefore, it is becoming important to generate oligosaccharide library of various sizes. In this regard, our present study may be the initial step for such a future study.

In conclusion, our approach using an octasaccharide library prepared *in vitro* appears to be useful for defining the specific structures required for binding various heparin-binding proteins. Furthermore, more divergent oligosaccharide libraries will be generated by the combined use of various HS modification enzymes such as other HS6ST isoforms and acceptor oligosaccharides of various sizes, and these oligosaccharides may allow more selective regulation of growth factor activities (see "Addendum"). In fact, the potential of such oligosaccharide libraries, containing mixed 2-*O*- and 6-*O*-sulfate substituents, has been demonstrated recently in analysis of sequence requirements for saccharides interacting with FGF-1 and FGF-2 (50).

Acknowledgments—We thank Drs. Hidenao Toyoda and Toshihiko Toida and Prof. Toshio Imanari (Faculty of Pharmaceutical Sciences, Chiba University, Chiba, Japan) for setting up a reversed-phase ion-pair chromatography system with sensitive and specific postcolumn detection. We also thank Prof. Ulf Lidahl (Department of Medical Biochemistry and Microbiology, Uppsala University, The Biomedical Center, Uppsala, Sweden) for exchanging the recent information on HS octasaccharide library and for useful discussions.

Addendum—During the review process of this manuscript, we reviewed the recent paper by Allen and Rapraeger (49) describing that HS structural requirements distinct from those for FGF binding are identified for both complex formation and signaling for each FGF and FGF receptor pair, which suggests the usefulness of the HS oligosaccharide library with longer chain sizes which we are going to generate.

REFERENCES

1. Conrad, H. E. (1998) *Heparin-Binding Proteins*, pp. 1–60, Academic Press, Inc., New York
2. David, G. (1993) *FASEB J.* **7,** 1023–1030
3. Yanagishita, M., and Hascall, V. C. (1992) *J. Biol. Chem.* **267,** 9451–9454
4. Aviezer, D., Hecht, D., Safran, M., Eisinger, M., David, G., and Yayon, A. (1994) *Cell* **79,** 1005–1013
5. Bernfield, M., Gotte, M., Park, P. W., Reizes, O., Fitzgerald, M. L., Lincecum, J., and Zako, M. (1999) *Annu. Rev. Biochem.* **68,** 729–777
6. Folkman, J., Klagsbrun, M., Sasse, J., Wadzinski, M., Ingber, D., and Vlodavsky, I. (1988) *Am. J. Pathol.* **130,** 393–400
7. Kjellen, L., and Lindahl, U. (1991) *Annu. Rev. Cell Biol.* **60,** 443–475
8. Rapraeger, A. C. (1993) *Curr. Opin. Cell Biol.* **5,** 844–853
9. Nakato, H., and Kimata, K. (2002) *Biochim. Biophys. Acta* **1573,** 312–318
10. Grobe, K., Ledin, J., Ringvall, M., Holmborn, K., Forsberg, E., Esko, J. D., and Kjellen, L. (2002) *Biochim. Biophys. Acta* **1573,** 209–215
11. HajMohammadi, S., Enjyoji, K., Princivalle, M., Christi, P., Lech, M., Beeler, D., Rayburn, H., Schwartz, J. J., Barzegar, S., de Agostini, A. I., Post, M. J., Rosenberg, R. D., and Shworak, N. W. (2003) *J. Clin. Investig.* **111,** 989–999
12. Bullock, S. L., Fletcher, J. M., Beddington, R. S., and Wilson, V. A. (1998) *Genes Dev.* **12,** 1894–1906
13. Orellana, A., Hirschberg, C. B., Wei, Z., Swiedler, S. J., and Ishihara, M. (1994) *J. Biol. Chem.* **269,** 2270–2276
14. Eriksson, I., Sandback, D., Ek, B., Lindahl, U., and Kjellen, L. (1994) *J. Biol. Chem.* **269,** 10438–10443
15. Aikawa, J., and Esko, J. D. (1999) *J. Biol. Chem.* **274,** 2690–2695
16. Aikawa, J., Grobe, K., Tsujimoto, M., and Esko, J. D. (2001) *J. Biol. Chem.* **276,** 5876–5882
17. Li, J.-P., Hagner-McWhirter, A., Kjellen, L., Jaan Palgi, M. J., and Lindahl, U. (1997) *J. Biol. Chem.* **272,** 28158–28163
18. Kobayashi, M., Habuchi, H., Yoneda, M., Habuchi, O., and Kimata, K. (1997) *J. Biol. Chem.* **272,** 13980–13985
19. Habuchi, H., Kobayashi, M., and Kimata, K. (1998) *J. Biol. Chem.* **273,** 9208–9213
20. Habuchi, H., Tanaka, M., Habuchi, O., Yoshida, K., Suzuki, H., Ban, K., and Kimata, K. (2000) *J. Biol. Chem.* **275,** 2859–2868
21. Liu, J., Shworak, N. W., Sinay, P., Schwartz, J. J., Zhang, L., Fritze, L. M., and Rosenberg, R. D. (1999) *J. Biol. Chem.* **274,** 5185–5192
22. Shworak, N. W., Liu, J., Petros, L. M., Zhang, L., Kobayashi, M., Copeland, N. G., Jenkins, N. A., Rosenberg, R. D., Eriksson, I., Sandback, D., Ek, B., Lindahl, U., and Kjellen, L. (1999) *J. Biol. Chem.* **274,** 5170–5184
23. Turnbull, J. E., Fernig, D. G., Ke, Y., Wilkinson, M. C., and Gallagher, J. T. (1992) *J. Biol. Chem.* **267,** 10337–10341
24. Habuchi, H., Suzuki, S., Saito, T., Tamura, T., Harada, T., Yoshida, K., and Kimata, K. (1992) *Biochem. J.* **285,** 805–813
25. Guimond, S., Maccarana, M., Olwin, B. B., Lindahl, U., and Rapraeger, A. C. (1993) *J. Biol. Chem.* **268,** 23906–23914
26. Ishihara, M. (1994) *Glycobiology* **4,** 817–824
27. Kreuger, J., Salmivirta, M., Sturiale, L., Gimenez-Gallego, G., and Lindahl, U. (2001) *J. Biol. Chem.* **276,** 30744–30752
28. Loo, B. M., and Salmivirta, M. (2002) *J. Biol. Chem.* **277,** 32616–32623
29. Lyon, M., Deakin, J. A., Mizuno, K., Nakamura, T., and Gallagher, J. T. (1994) *J. Biol. Chem.* **269,** 11216–11223
30. Ashikari, S., Habuchi, H., and Kimata, K. (1995) *J. Biol. Chem.* **270,** 29586–29593
31. Deakin, J. A., and Lyon, M. (1999) *J. Cell Sci.* **112,** 1999–2009
32. Feyzi, E., Lustig, F., Fager, G., Spillmann, D., Lindahl, U., and Salminirta, M. (1997) *J. Biol. Chem.* **272,** 5518–5524
33. Shively, J. E., and Conrad, H. E. (1976) *Biochemistry* **15,** 3932–3942
34. Thompson, J. D., Higgins, D. G., and Gibson, T. J. (1994) *Nucleic Acids Res.* **22,** 4673–4680
35. Toyoda, H., Kinoshita-Toyoda, A., and Selleck, S. B. (2000) *J. Biol. Chem.* **275,** 2269–2275
36. Plotnikov, A. N., Hubbard, S. R., Schlessinger, J., and Mohammadi, M. (2000) *Cell* **101,** 413–424
37. Luo, Y., Lu, W., Mohamedali, K. A., Jang, J. H., Jones, R. B., Gabriel, J. L., Kan, M., and McKeehan, W. L. (1998) *Biochemistry* **37,** 16506–16515
38. Raman, R., Venkataraman, G., Ernst, S., Sasisekharan, V., and Sasisekharan, R. (2003) *Proc. Natl. Acad. Sci. U. S. A.* **100,** 2357–2362
39. Faham, S., Hileman, R. E., Fromm, J. R., Linhardt, R. J., and Reed, D. C. (1996) *Science* **271,** 1116–1120
40. DiGabriele, A. D., Lax, I., Chen, D. I., Svahn, C. M., Jaye, M., Schlessinger, J., and Hendrickson, W. A. (1998) *Nature* **393,** 812–817
41. Lietha, D., Chirgadze, D. Y., Mulloy, B., Blundell, T. L., Gherardi, E., Ohuchi, H., Yoshioka, H., Tanaka, A., Kawakami, Y., Nohno, T., Noji, S., Shworak, N. W., Liu, J., Petros, L. M., Zhang, L., Kobayashi, M., Copeland, N. G., Jenkins, N. A., Rosenberg, R. D., Eriksson, I., Sandback, D., Ek, B., Lindahl, U., and Kjellen, L. (2001) *EMBO J.* **20,** 5543–5555
42. Paine-Saunders, S., Viviano, B. L., Zupicich, J., Skarnes, W. C., and Saunders, S. (2000) *Dev. Biol.* **225,** 179–187
43. Grisaru, S., Cano-Gauci, D., Tee, J., Filmus, J., and Rosenblum, N. D. (2001) *Dev. Biol.* **231,** 31–46
44. Fujise, M., Takeo, S., Kamimura, K., Matsuo, T., Aigaki, T., Izumi, S., and Nakato, H. (2003) *Development* **130,** 1515–1522
45. Fujise, M., Izumi, S., Selleck, S. B., and Nakato, H. (2001) *Dev. Biol.* **235,** 433–448
46. Selleck, S. B. (2000) *Trends Genet.* **16,** 206–212
47. Ohkawara, B., Iemura, S., ten Dijke, P., and Ueno, N. (2002) *Curr. Biol.* **12,** 205–209
48. Reddi, A. H. (1998) *Nat. Biotechnol.* **16,** 247–252
49. Allen, B. L., and Rapraeger, A. C. (2003) *J. Cell Biol.* **163,** 637–648
50. Jemth, P., Kreuger, J., Kusche-Gullberg, M., Sturiale, L., Gimenez-Gallego, G., and Lindahl, U. (2002) *J. Biol. Chem.* **277,** 30567–30573

Minireview

THE JOURNAL OF BIOLOGICAL CHEMISTRY
Vol. 279, No. 37, Issue of September 10, pp. 38079–38082, 2004

Inter-α-trypsin Inhibitor, a Covalent Protein-Glycosaminoglycan-Protein Complex*

Published, JBC Papers in Press, May 19, 2004,
DOI 10.1074/jbc.R300039200

Lisheng Zhuo‡§, Vincent C. Hascall¶, and Koji Kimata‡‖

From the ‡Institute for Molecular Science of Medicine, Aichi Medical University, Nagakute, Aichi 480-1195, Japan, §CREST, Japan Science and Technology Agency, Kawaguchi, Saitama 560-0082, Japan, and ¶Department of Biomedical Engineering and Orthopaedic Research Center/ND20, The Cleveland Clinic Foundation, Cleveland, Ohio 44195

The inter-α-trypsin inhibitor (IαI)[1] family, a typical and classical example for protein-glycosaminoglycan-protein (PGP) complexes, occurs constitutively in plasma at relatively high concentrations and is a result of alternate combinations of three kinds of heavy chains with a common light chain, the bikunin proteoglycan. The family is characterized by the unique covalent linkage between the heavy chains and the chondroitin sulfate chain of bikunin. The early studies on the IαI family molecules have largely focused on the light chain (bikunin) that is fully responsible for their protease inhibitory activity. Since the mid-1980s, the structures of the family molecules have been clarified, and this led to the discovery of their complex interaction with another glycosaminoglycan, hyaluronan (HA), generating the serum-derived hyaluronan-associated protein (SHAP)-HA complex. Research from various directions has clarified many aspects of the biological function of the PGP complexes and provides a new vista on their interesting structure-function relationships, especially on their roles in inflammation.

Emergence of the Inter-α Inhibitor Family

The IαI family was first identified as a trypsin inhibitor activity in nephropathic and pneumonopathic urine in 1909 and in normal urine in 1910. One member, the urinary trypsin inhibitor (UTI), was purified much later in the 1950s (1, 2) when it was independently isolated by researchers working on mucopolysaccharides, leukemia, and urolithiasis and was given many names: acid-stable protease inhibitor, prealbumin-like protease inhibitor, urinastatin, HI30, mingin, EDC1, uronic acid-rich protein, and nephrocalin (3–5). Based on the presence of two tandem Kunitz-type protease inhibitory domains, a structure-based name, bikunin, was suggested in 1990 to avoid confusion (6). It is now known that bikunin (M_r ~ 40,000) is a proteoglycan with a chondroitin sulfate (CS) chain and is the predominant protease inhibitor in urine. Bikunin is acid- and heat-stable and has an acidic pI between 2 and 3 largely due to the presence of sialic acid and CS.

There were continuous efforts to find a serum cognate based on a hypothesis that UTI has a serum origin. In the 1970s, this led to the identification of serum IαI (7), a macromolecule previously purified in the 1960s (8) (Fig. 1). Conclusive evidence for the identity came from the comparison of amino acid sequences in the 1980s (9). Smaller components with inhibitor activity were released when IαI was treated *in vitro* in acidic conditions or with proteases, such as plasmin, trypsin, and elastase (10, 11), or when incubated with inflammatory cells, in particular neutrophils, or cancer cells (12, 13). Cognate molecules with lower molecular weights were also found in serum, pre-α inhibitor (PαI), and inter-α-like trypsin inhibitor (14).

IαI was thought to be a single polypeptide chain until molecular biology techniques became available. Cell-free translation of liver mRNAs (15) and subsequent cloning (16) indicated that IαI contains "heavy" and "light" polypeptides encoded by distinct genes. Reviews in 1990 summarized the multipeptide chain structure and defined the IαI family (6, 17). IαI family molecules are encoded by at least five genes, *ITIH1–ITIH4* for the four heavy chains (HCs) and *AMBP* for the light chain (the core protein of bikunin). Interestingly, the *AMBP* gene encodes both the core protein and a functionally unrelated serum protein, α_1-microglobulin, as a precursor fusion protein (18). cDNAs of the four HCs show high sequence homology except in the C-terminal one-third of HC4 (19).

Structure and Synthesis of IαI Family Molecules

The multipeptide structure of IαI was masked by its unusual PGP structure in which the polypeptide subunits are covalently linked together via a CS chain (20). In 1981, the UTI carbohydrates were identified as: (*a*) an *O*-linked, GalNAc-rich chain attached to serine at position 10 and (*b*) an *N*-linked oligosaccharide at position 45 (21). Chondroitinase and testicular hyaluronidase digestion of IαI and PαI identified the *O*-glycan as a low sulfated CS chain (22, 23) and separated the HCs and bikunin (14, 24). The CS linkage to bikunin is a typical *O*-xylosylserine (22). Analyses also identified the novel ester bond that links the α-carboxyl of C-terminal aspartates of the HCs with C-6 hydroxyl groups of internal GalNAcs in the CS chain (20, 25) (Fig. 1). The amino acid sequence at the CS attachment site in bikunin, Glu-Gly-Ser-Gly, is well conserved among all species examined. The CS chain is relatively short (M_r ~ 8000), with 12–18 disaccharide repeats (GlcUAβ1,3-GalNAcβ1,4-) and a conventional linkage region (GlcUAβ1–3Galβ1–3Galβ1–4Xylβ1)-*O*-Ser (26, 27). About 30% of the GalNAc, usually those near the linkage region, are sulfated at C-4 hydroxyl groups (27). CS chains synthesized during inflammations are shorter with decreased sulfation (28). In the electron microscope, bikunin appears as a small sphere (diameter of ~2 nm), whereas HCs have an N-terminal globule (diameter of ~11 nm) with a thin tail (length of ~15.5 nm) attached to the bikunin sphere (29). The two HCs of human IαI are located close to each other in the less sulfated region of the CS chain (27).

The HCs on IαI vary from species to species. Typically, human IαI contains HC1 and HC2 (14), bovine IαI contains HC2 and HC3 (30), and rodent IαI contains both types (31). On the other hand, the single HC in PαI is HC3 in all species examined except for bovine PαI, which contains HC2 (30). Low levels of HC2/bikunin (inter-α-like trypsin inhibitor) and HC1/bikunin are found in human serum, which seem to be degraded forms of IαI (14, 25). Currently, neither the reason nor the mechanism for the selectivity of HCs is known.

Although IαI family genes are expressed in various tissues (32), the circulating IαI family molecules are produced principally by the liver. Interestingly, bikunin and HC cDNA cotransfection shows that cells other than hepatocytes, COS cells, also can couple a HC with the bikunin proteoglycan (33). Bikunin is first synthesized in fusion with α_1-microglobulin (34), and the cleavage occurs in the *trans*-Golgi after adding the CS and HCs (35). The connecting tetrapeptide (Arg-X_1-X_2-Arg) conforms to a consensus sequence recognized by the intracellular endoprotease family that includes

* This minireview will be reprinted in the 2004 Minireview Compendium, which will be available in January, 2005. This work was supported in part by a grant-in-aid for scientific research (B) from the Japan Society for the Promotion of Science and by a special research fund from Seikagaku Corporation.

‖ To whom correspondence should be addressed. Tel.: 81-52-264-4811 (ext. 2088); Fax: 81-561-63-3532; E-mail: kimata@amugw.aichi-med-u.ac.jp.

[1] The abbreviations used are: IαI, inter-α-trypsin inhibitor; UTI, urinary trypsin inhibitor; PαI, pre-α inhibitor; HC, heavy chain of IαI family molecules; PGP, protein-glycosaminoglycan-protein covalent complex; SHAP, serum-derived hyaluronan-associated protein; HA, hyaluronan; CS, chondroitin sulfate; TSG6 or TNFIP6, tumor necrosis factor-stimulated gene 6.

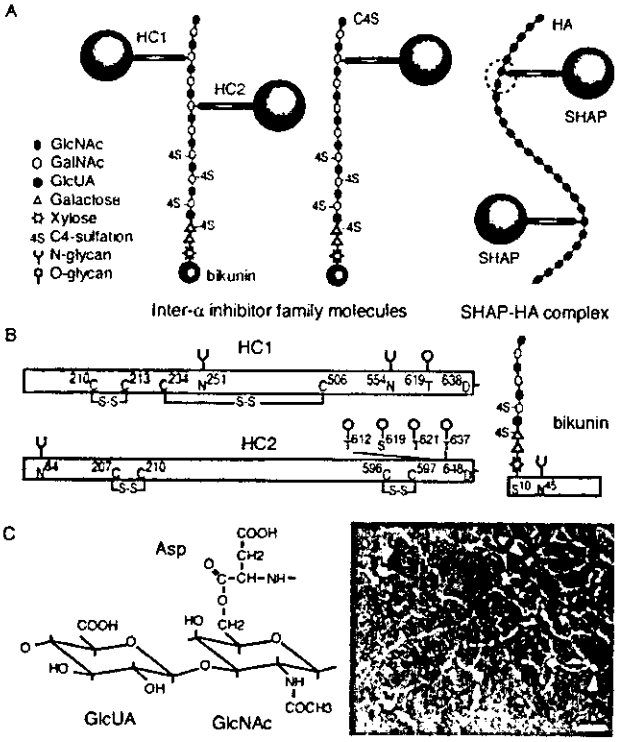

FIG. 1. **Protein-glycosaminoglycan-protein complex.** *A*, schematic structure of IαI family molecules and the SHAP-HA complex. The HCs/SHAPs are covalently linked together by the CS-4-sulfate (*C4S*) chain of the bikunin proteoglycan or by HA. *B*, structures of the HCs and bikunin. *Forks* and *spoons* represent *N*-linked sugars and *O*-linked sugars, respectively (adapted from Refs. 27, 29, and 77). *C*, structure of the SHAP-HA linkage region (*dashed circle* in *A*). The photograph shows negative stained electron micrographic images of the SHAP-HA complex (73). HA is visualized as a fibrous network and SHAP as globular structures (*arrows* and *arrowheads*) with a thin tail that attaches to HA (*arrows*). The morphology matches that of IαI heavy chains reported previously (29). The *bar* represents 20 nm. The portions involved in the formation of globular structures of heavy chains are marked *gray* in *B*. The portion corresponding to the two Kunitz domains of bikunin is also marked in *B*.

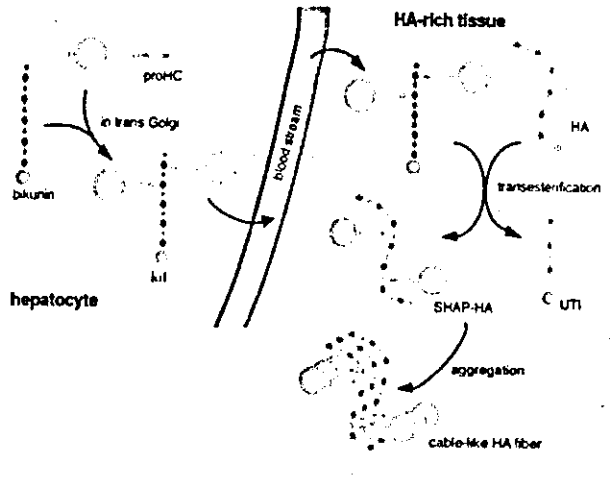

FIG. 2. **A model for the structure and function relation of a PGP complex.** The IαI family molecules are synthesized in hepatocytes, where one or two HCs are linked to the CS chain of bikunin in the Golgi apparatus. Upon a proper stimulus, the molecules are recruited to extravascular sites, where the HCs are transferred to the locally synthesized HA to form the SHAP-HA complexes (transesterification), which play roles in construction of extracellular matrices by aggregating into a "cable-like structure" containing the complexes and in interaction of the matrices with inflammatory cells.

furin. However, furin does not seem to be responsible for the cleavage (36).

The HCs undergo several proteolytic steps during biosynthesis. The signal and following N-terminal propeptides (19) are removed in the endoplasmic reticulum, probably by a Golgi enzyme in transit (37, 38). The large C-terminal extension (240–280 amino acid residues beginning with the conserved sequence Pro-His-Phe-Ile-Ile) is released when the remainder of the HC is coupled to the CS (Fig. 2) (19). Therefore, the assembly of a HC involves two likely coordinated steps: a cleavage of the Asp-Pro bond and then the formation of the ester bond (38). The C-terminal extension seems to be required for the formation of the ester linkage (37). No protease with specificity toward the conserved sequence around the cleavage site has been described.

Protease Inhibitor Activity of IαI Family Molecules

As their original names suggest, the family molecules were studied extensively as protease inhibitors. Bikunin exhibits a weak inhibitory activity against proteases including trypsin, chymotrypsin, neutrophil elastase, and plasmin (39). However, none has been defined as a physiological target of bikunin, which questions whether protease inhibition is a major function of IαI family molecules. Although circulating levels are high (150–500 μg/ml), they account for only ~5% of the total protease inhibitory activity of the plasma, and the K_i values of bikunin are not low enough to be effective at physiological concentrations (39). Proteases that bikunin inhibits are often more efficiently inhibited by their respective physiological inhibitors (40). Accordingly, on the basis of clearance of injected bikunin-protease complexes, it was proposed that the IαI family functions as a shuttle that traps proteases and then transfers them to physiological inhibitors (41). However, bikunin inhibits plasmin on the surfaces of cancer cells more efficiently than plasmin in solution, in contrast to α_2-macroglobulin and α_1-inhibitor, which may relate to the antimetastatic effect of bikunin (42). In addition, bikunin may also inhibit granzyme K, the lymphocyte granule-stored serine protease that is implicated in T-cell- and natural killer cell-mediated cytotoxic defense after recognition of target cells (43). Trypstatin, an inhibitor of chymase secreted by peritoneal mast cells, was suggested to be a processed fragment of bikunin that the cells had taken up from the circulation (44). Other diverse activities, particularly pharmaceutical effects, of bikunin have been described, such as mitogenic activity, inhibitory activity toward hyaluronidase, prevention from premature delivery, ischemia stress and renal failure, and suppression of pancreatitis, colitis, and arthritis, for which various mechanisms have been proposed (for review, see Ref. 45).

The above studies focused on the bikunin portion of IαI family molecules. However, more than 90% of circulating bikunin carries HCs, whereas urinary bikunin is predominantly free of HCs (46). Furthermore, free bikunin has a much shorter half-life in circulation (4 min in mice) than that of HC-bikunin complexes (several hours in mice) (47, 48). This paradox is explained by recent studies of IαI-HA interactions.

SHAP-HA Complex and Its Synthesis

Soon after its discovery in the 1960s, IαI was found to have an association with HA (49, 50). HA is the major glycosaminoglycan in synovial fluid that is responsible for its viscoelastic properties and joint-lubricating function. HA isolated from knee joints of patients with active rheumatoid arthritis or chronic gout contained more firmly bound protein (~10%) than HA from normal knee joints (~2%). Immunodiffusion with specific antibodies identified the protein as IαI then thought to be a single protein (50). The pathological HA preparations had altered properties, such as gel formation, electrophoretic immobility, and extremely rapid sedimentation in the ultracentrifuge at pH 4.5, suggesting an aggregation of the protein-HA complex (50). These investigators proposed that IαI entered the diseased joint from serum and became firmly bound to HA, thereby altering its properties (50, 51). These pioneering findings were neglected except in a report in 1988 that confirmed the pathological association of IαI with synovial HA and further showed that the complex was more resistant to degradation by oxygen-derived free radicals (52).

In 1990, a protein of ~85 kDa was found firmly associated with HA in the extracellular matrix of cultured mouse dermal fibroblasts (53). The protein was not metabolically labeled and therefore was derived from the serum added to the culture. It was designated SHAP and was identified as the HCs of the IαI family molecules (54). The term SHAP is used below for HCs in HA complexes.

The SHAP-HA complexes were then isolated from synovial fluid

and from preovulatory follicular fluid (55). Mass spectrometry showed that SHAPs are bound to HA by an ester bond between carboxyl groups of the aspartates at their C termini and the C-6 hydroxyl groups of internal *N*-acetylglucosamines in HA, analogous to the original HC ester bond to CS in IαI (56) (Fig. 1). Because several SHAPs are linked to one HA molecule, the SHAP-HA complex is a second PGP covalent complex. The analogous linkage structures in the SHAP-HA complex and IαI suggest that the SHAP-HA complex is formed by a transesterification of HCs from CS to HA, accompanied by the release of bikunin proteoglycan (Fig. 2).

SHAP-HA complex formed when HA and IαI were incubated with serum at 37 °C (53, 56). No HC transfer was observed at low temperature or when divalent cations were absent, indicating the presence of an as yet unidentified enzymatic factor (53, 54). HC transfer activity has also been detected in follicular fluid and in media conditioned by follicular granulosa cells, hepatoma cells, or glioma cells (57, 58).[2] Recently, tumor necrosis factor stimulated gene-6 product (TSG6, also named TNFIP6) has been identified as a candidate because it interacts with both HA through its link module (59) and IαI (60). Furthermore, TSG6-null mice exhibit the same phenotype as bikunin-null mice, namely inability to form the SHAP-HA complex and hence to form the expanded HA-based matrix of the cumulus oöphorus during ovulation, with resulting female infertility (47, 61). Interestingly, recombinant TSG6 forms an ~120-kDa complex with IαI, in which TSG6 appears to replace a HC on the CS (60). This complex was present in arthritic synovial fluid and air pouch exudates (62). Although it was suggested that TSG6 acts as an enhancing factor rather than as the transfer activity *per se* (63), recent work has shown that TSG6 can displace HC from IαI to form a TSG6-HC complex in solution that can in turn form a SHAP-HA complex when HA or HA oligosaccharides are added (64). Further, PG-M/versican, a HA-binding proteoglycan with two tandem link modules, enhances the formation of the SHAP-HA complex in solution (65).

Matrix-stabilizing Effect of the SHAP-HA Complex

In the pre-ovulatory mammalian follicle, the oocyte is closely surrounded by ~1000 cumulus cells in a compact cumulus cell-oocyte complex. After an ovulatory stimulus, the follicle becomes permeable to serum, introducing IαI, and the cumulus cells begin to synthesize HA and organize it into an extensive extracellular matrix, causing a dramatic increase in cell-oocyte complex volume (cumulus oöphorus expansion). Compact cell-oocyte complexes expand *in vitro* when incubated in the presence of follicle-stimulating hormone and serum. In the absence of serum, HA is synthesized but not organized into a matrix. The necessary serum factor was identified as IαI, and it was suggested that the mechanism involved a direct ionic interaction between IαI and HA (66). However, the interaction was weak at physiological ionic strength, questioning its ability to maintain the matrix structure. Further, HA isolated from ovarian follicular fluid contained HCs, but no bikunin, indicating that a SHAP-HA complex is formed (55, 60, 64). Serum from the bikunin-null mouse contains unprocessed HCs, but they are not able to form the SHAP-HA complex (47). Consequently, homozygous null female mice are defective in cumulus oöphorus expansion, with greatly reduced oocyte ovulation and subsequent infertility. Fertilization was rescued by intraperitoneal administration of purified IαI but not by bikunin alone (47). Incubation of bikunin proteoglycan with serum from homozygous null mice also failed to couple it with the unprocessed HCs, consistent with the fact that the assembly of IαI is completed in the Golgi apparatus of hepatocytes (35). These results suggest a novel concept for the function of bikunin proteoglycan, *i.e.* to provide a CS chain to form an ester bond with HCs for their subsequent transfer to HA.

TSG6 synthesis is also up-regulated in cumulus cells and in surrounding granulosa cells in the preovulatory follicle (67, 68). Further, hyaluronidase digestion of the expanded cumulus oöphorus identified covalent TSG6-SHAP-HA complexes as well as SHAP-HA complexes in the expanded matrix, whereas bikunin was absent (68). Conversely, hyaluronidase digestion of ovaries from the TSG6-null mouse revealed a complete absence of SHAP-HA complexes (61). Thus, TSG6 is essential for the transesterification of HCs from IαI in organizing the expanded cumulus oöphorus matrix. The TSG6-SHAP-HA complex provides a possible mechanism for stabilizing the matrix by cross-linking HA between the non-covalent TSG6-HA interaction, mediated by the link module in TSG6, and the covalent cross-link of its HA-SHAP partner.

IαI family molecules also exert matrix-stabilizing effects on cultured human fibroblasts, on human mesothelial cells (69), and on mouse mammary carcinoma cells (70), likely through SHAP-HA complexes. HA and IαI normally distribute in different body compartments, connective tissues and the circulation, respectively. Their convergence under various abnormal conditions, such as malignancy and inflammation, and during some physiological processes, such as ovulation, is associated with increased bikunin levels in urine (71). Therefore, the function of the interactions involving IαI and HA is of general relevance.

SHAP-HA Complex in Inflammatory Diseases

Rheumatoid Arthritis—The synovium, a highly vascularized tissue lacking a basement membrane-like structure, allows synoviocyte-secreted HA to enter the joint cavity where it is a major component of the synovial fluid. An inflamed synovium is the most likely site for the formation of the synovial SHAP-HA complex. Indeed, the SHAP-HA complex was detected within the synovial cavity at a concentration far higher than that in the circulation (72, 73). The complex from rheumatoid arthritic synovial fluid is heterogeneous in HA chain length and in the SHAP-to-HA molecular ratio: a HA chain of ~2 MDa carries 3–5 SHAP proteins on average (73). Some altered properties of pathological synovial HA, such as gelation at low pH and rapid sedimentation upon ultracentrifugation (49, 50), and the ability to form a macromolecular aggregate (73) may relate to the presence of SHAPs. These results and those discussed below suggest that the SHAP-HA complex has a role in the inflammatory response by regulating adhesion of infiltrating leukocytes.

Inflammatory Bowel Disease—Crohn's disease and ulcerative colitis are the major chronic inflammatory diseases of the gastrointestinal tract and are often referred to as inflammatory bowel disease. The major pathological changes include an increase in intestinal mucosal mononuclear leukocytes and a dramatic hyperplasia of the smooth muscle cells of the muscularis mucosae. The etiology of inflammatory bowel disease is multifactorial including viral infection. The interaction between inflamed smooth muscle cells and recruited leukocytes is also important in the development and propagation of this disease. Studies *in vitro* showed that viral infection of human colon smooth muscle cells or treatment with the virus mimetic polyinosinic acid:polycytidylic acid up-regulated the production of HA and the formation of extracellular HA "cable" structures (74) (Fig. 2). The cable structures were specifically formed in the presence of serum, and the SHAP-HA complex was found in the structure (74). Cell adhesion assays revealed that peripheral mononuclear cells or histiocytic lymphoma U937 monocytic cells bound specifically to the cables via a mechanism involving in part CD44, a HA receptor, on their surface. Therefore, a highly organized structure, involving the SHAP-HA complex, may be required for the leukocytes to adhere and potentially to subsequently activate.

Serum Levels of the SHAP-HA Complex—It is generally accepted that HA is partially degraded at local sites and carried by lymph to the lymph nodes where a large portion is endocytosed and degraded. However, a significant portion is also carried to the general circulation and rapidly cleared by liver sinusoidal endothelial cells. The daily turnover of HA is in the order of 10–100 mg whereas the level in circulation is maintained at only about 30–40 ng/ml in healthy individuals (75). However, under pathological conditions, up-regulated production, impaired uptake, and/or decreased degradation cause dramatic elevation of serum HA. Clinically, the level is used to aid diagnosis and to monitor progress in cases of rheumatoid arthritis and liver cirrhosis (76). An enzyme-linked immunosorbent assay method, developed for measuring the level of the SHAP-HA complex in serum and other humoral sources (72), has revealed a significant correlation between the levels of HA and SHAP in diseases with elevated serum HA (72, 73)[2] and provides

[2] L. Zhuo, V. C. Hascall, and K. Kimata, unpublished observations.

further evidence for the formation of the SHAP-HA complex in these pathological conditions.

Concluding Remarks

For a long period, studies on IαI family molecules focused on bikunin, the protease inhibitor, with the impression that the HCs only modified the function of bikunin. After the SHAP-HA complex was identified in 1990, a matrix-stabilizing role of IαI family molecules was observed, and its biological relevance was established with mouse models in 2001. These studies provide a novel concept for the role of each domain of IαI, *i.e.* the HCs are directly related to the physiological function of IαI through transfer to HA, and their coupling to bikunin is necessary for the transesterification reaction. It is now important to find if other partners interact with the HCs in addition to HA, TSG6, and PG-M/versican (64, 70). Characterization of potentially functional motifs in the HC polypeptide, such as those suggested by sequence homology (19), will also be useful. Finally, the mechanisms for forming the HC-CS bond in IαI in the Golgi of hepatocytes and for the transesterification to form the SHAP-HA counterpart needed to be defined in both normal processes such as TSG6-mediated cumulus oöphorus expansion, and in pathological processes such as rheumatoid arthritis and inflammatory bowel disease.

Acknowledgments—We are very much indebted to people who have been involved in this research.

REFERENCES

1. Shulman, N. R. (1955) *J. Biol. Chem.* **213,** 655–671
2. Astrup, T., Alkjoer, K., and Soardi, F. (1959) *Scand. J. Clin. Lab. Invest.* **11,** 181
3. Anderson, A. J., and Maclagan, N. F. (1955) *Biochem. J.* **59,** 638–644
4. Chawla, R. K., Wadsworth, A.D., and Rudman, D. (1978) *J. Immunol.* **121,** 1636–1639
5. Atmani, F., Mizon, J., and Khan, S. R. (1996) *Eur. J. Biochem.* **236,** 984–990
6. Gebhard, W., Hochstrasser, K., Fritz, H., Enghild, J. J., Pizzo, S. V., and Salvesen, G. (1990) *Biol. Chem. Hoppe Seyler* **371,** (suppl.) 13–22
7. Proksch, G. J., Lane, J., and Nordschow, C. D. (1973) *Clin. Biochem.* **6,** 200–206
8. Heide, K., Heimburger, N., and Haupt, H. (1965) *Clin. Chim. Acta* **11,** 82
9. Wachter, E., and Hochstrasser, K. (1981) *Hoppe Seyler's Z. Physiol. Chem.* **362,** 1351–1355
10. Dietl, T., Dobrinski, W., and Hochstrasser, K. (1979) *Hoppe Seyler's Z. Physiol. Chem.* **360,** 1313–1318
11. Pratt, C. W., and Pizzo, S. V. (1987) *Biochemistry* **26,** 2855–2863
12. Pratt, C. W., Swaim, M. W., and Pizzo, S. V. (1989) *J. Leukocyte Biol.* **45,** 1–9
13. Kobayashi, H., Gotoh, J., Hirashima, Y., and Terao, T. (1996) *J. Biol. Chem.* **271,** 11362–11367
14. Enghild, J. J., Thogersen, I. B., Pizzo, S. V., and Salvesen, G. (1989) *J. Biol. Chem.* **264,** 15975–15981
15. Bourguignon, J., Vercaigne, D., Sesboue, R., Martin, J. P., and Salier, J. P. (1983) *FEBS Lett.* **162,** 379–383
16. Diarra-Mehrpour, M., Bourguignon, J., Sesboue, R., Mattei, M.G., Passage, E., Salier, J.P., and Martin, J.P. (1989) *Eur. J. Biochem.* **179,** 147–154
17. Salier, J. P. (1990) *Trends Biochem. Sci.* **15,** 435–439
18. Kaumeyer, J. F., Polazzi, J. O., and Kotick, M. P. (1986) *Nucleic Acids Res.* **14,** 7839–7850
19. Chan, P., Risler, J. L., Raguenez, G., and Salier, J. P. (1995) *Biochem. J.* **306,** 505–512
20. Enghild, J. J., Salvesen, G., Hefta, S. A., Thogersen, I. B., Rutherfurd, S., and Pizzo, S. V. (1991) *J. Biol. Chem.* **266,** 747–751
21. Hochstrasser, K., Schonberger, O. L., Rossmanith, I., and Wachter, E. (1981) *Hoppe Seyler's Z. Physiol. Chem.* **362,** 1357–1362
22. Balduyck, M., Mizon, C., Loutfi, H., Richet, C., Roussel, P., and Mizon, J. (1986) *Eur. J. Biochem.* **158,** 417–422
23. Ochiai, H., Toyoda, H., Onodera, M., Shinbo, A., Shinomiya, K., and Imanari, T. (1988) *Chem. Pharm. Bull. (Tokyo)* **36,** 3726–3727
24. Jessen, T. E., Faarvang, K. L., and Ploug, M. (1988) *FEBS Lett.* **230,** 195–200
25. Enghild, J. J., Salvesen, G., Thogersen, I. B., Valnickova, Z., Pizzo, S. V., and Hefta, S. A. (1993) *J. Biol. Chem.* **268,** 8711–8716
26. Toyoda, H., Kobayashi, S., Sakamoto, S., Toida, T., and Imanari, T. (1993) *Biol. Pharm. Bull.* **16,** 945–947
27. Enghild, J. J., Thogersen, I. B., Cheng, F., Fransson, L. A., Roepstorff, P., and Rahbek-Nielsen, H. (1999) *Biochemistry* **38,** 11804–11813
28. Capon, C., Mizon, C., Lemoine, J., Rodie-Talbere, P., and Mizon, J. (2003) *Biochimie (Paris)* **85,** 101–107
29. Blom, A.M., Morgelin, M., Oyen, M., Jarvet, J., and Fries, E. (1999) *J. Biol. Chem.* **274,** 298–304
30. Castillo, G. M., and Templeton, D. M. (1993) *FEBS Lett.* **318,** 292–296
31. Yamamoto, T., Yamamoto, K., and Sinohara, H. (1996) *J. Biochem. (Tokyo)* **120,** 145–152
32. Mizushima, S., Nii, A., Kato, K., and Uemura, A. (1998) *Biol. Pharm. Bull.* **21,** 167–169
33. Blom, A. M., Thuveson, M., and Fries, E. (1997) *Biochem. J.* **328,** 185–191
34. Lindqvist, A., Bratt, T., Altieri, M., Kastern, W., and Akerstrom, B. (1992) *Biochim. Biophys. Acta* **1130,** 63–67
35. Bratt, T., Olsson, H., Sjoberg, E. M., Jergil, B., and Akerstrom, B. (1993) *Biochim. Biophys. Acta* **1157,** 147–154
36. Brat, T., Cedervall, T., and Akerstrom, B. (1994) *FEBS Lett.* **354,** 57–61
37. Thuveson, M., and Fries, E. (1999) *J. Biol. Chem.* **274,** 6741–6746
38. Thogersen, I.B., and Enghild, J. J. (1995) *J. Biol. Chem.* **270,** 18700–18709
39. Potempa, J., Kwon, K., Chawla, R., and Travis, J. (1989) *J. Biol. Chem.* **264,** 15109–15114
40. Odum, L. (1991) *Dan. Med. Bull.* **38,** 68–77
41. Pratt, C. W., and Pizzo, S. V. (1986) *Arch. Biochem. Biophys.* **248,** 587–596
42. Kobayashi, H., Shinohara, H., Takeuchi, K., Itoh, M., Fujie, M., Saitoh, M., and Terao, T. (1994) *Cancer Res.* **54,** 844–849
43. Wilharm, E., Parry, M. A., Friebel, R., Tschesche, H., Matschiner, G., Sommerhoff, C. P., and Jenne, D. E. (1999) *J. Biol. Chem.* **274,** 27331–27337
44. Itoh, H., Ide, H., Ishikawa, N., and Nawa, Y. (1994) *J. Biol. Chem.* **269,** 3818–3822
45. Fries, E., and Blom, A. M. (2000) *Int. J. Biochem. Cell Biol.* **32,** 125–137
46. Slota, A., Sjoquist, M., Wolgast, M., Alston-Smith, J., and Fries, E. (1994) *Biol. Chem. Hoppe Seyler* **375,** 127–133
47. Zhuo, L., Yoneda, M., Zhao, M., Yingsung, W., Yoshida, N., Kitagawa, Y., Kawamura, K., Suzuki, T., and Kimata, K. (2001) *J. Biol. Chem.* **276,** 7693–7696
48. Sugiki, M., Sumi, H., Maruyama, M., Yoshida, E., and Mihara, H. (1989) *Enzyme* **42,** 31–38
49. Hamerman, D., and Sandson, J. (1963) *J. Clin. Invest.* **42,** 1882–1889
50. Sandson, J., Hamerman, D., and Schwick, G. (1965) *Trans Assoc. Am. Physicians* **78,** 304–313
51. Becker, A., and Sandson, J. (1971) *Arthritis Rheum.* **14,** 764–766
52. Hutadilok, N., Ghosh, P., and Brooks, P. M. (1988) *Ann. Rheum. Dis.* **47,** 377–385
53. Yoneda, M., Suzuki, S., and Kimata, K. (1990) *J. Biol. Chem.* **265,** 5247–5257
54. Huang, L., Yoneda, M., and Kimata, K. (1993) *J. Biol. Chem.* **268,** 26725–26730
55. Jessen, T. E., Odum, L., and Johnsen, A. H. (1994) *Biol. Chem. Hoppe Seyler* **375,** 521–526
56. Zhao, M., Yoneda, M., Ohashi, Y., Kurono, S., Iwata, H., Ohnuki, Y., and Kimata, K. (1995) *J. Biol. Chem.* **270,** 26657–26663
57. Chen, L., Zhang, H., Powers, R. W., Russell, P. T., and Larsen, W. J. (1996) *J. Biol. Chem.* **271,** 19409–19414
58. Odum, L., Andersen, C. Y., and Jessen, T. E. (2002) *Reproduction* **124,** 249–257
59. Lee, T. H., Wisniewski, H. G., and Vilcek, J. (1992) *J. Cell Biol.* **116,** 545–557
60. Wisniewski, H.G., Burgess, W.H., Oppenheim, J.D., and Vilcek, J. (1994) *Biochemistry* **33,** 7423–7429
61. Fulop, C., Szanto, S., Mukhopadhyay, D., Bardos, T., Kamath, R. V., Rugg, M. S., Day, A. J., Salustri, A., Hascall, V. C., Glant, T. T., and Mikecz, K. (2003) *Development* **130,** 2253–2261
62. Wisniewski, H. G., Hua, J. C., Poppers, D. M., Naime, D., Vilcek, J., and Cronstein, B.N. (1996) *J. Immunol.* **156,** 1609–1615
63. Jessen, T. E., and Odum, L. (2003) *Reproduction* **125,** 27–31
64. Mukhopadhyay, D., Asari, A., Rugg, M. S., Day, A. J., and Fulop, C. (2004) *J. Biol. Chem.* **279,** 11119–11128
65. Yoneda, M., Zhao, M., Zhuo, L., Watanabe, H., Yamada, Y., Huang, L., Nagasawa, S., Nishimura, H., Shinomura, T., Isogai, Z., and Kimata, K. (2000) in *New Frontiers in Medical Sciences: Redefining Hyaluronan* (Abatangelo, G., and Weigel, P. H., eds) pp. 21–30, Elsevier Science B.V., Amsterdam
66. Chen, L., Mao, S. J., McLean, L. R., Powers, R. W., and Larsen, W. J. (1994) *J. Biol. Chem.* **269,** 28282–28287
67. Fulop, C., Kamath, R. V., Li, Y., Otto, J. M., Salustri, A., Olsen, B. R., Glant, T. T., and Hascall, V. C. (1997) *Gene (Amst.)* **202,** 95–102
68. Mukhopadhyay, D., Hascall, V. C., Day, A. J., Salustri, A., and Fulop, C. (2001) *Arch. Biochem. Biophys.* **394,** 173–181
69. Blom, A., Pertoft, H., and Fries, E. (1995) *J. Biol. Chem.* **270,** 9698–9701
70. Zhao, M., Yoneda, M., Zhuo, L., Huang, L., Watanabe, H., Yamada, Y., Nagasawa, S., Nishimura, H., and Kimata, K. (2002) in *Hyaluronan* (Kennedy, J. F., Phillips, G. O., Williams, P. A., and Hascall, V. C., eds) Vol. 1, pp. 497–500, Woodhead Publishing Ltd., Cambridge
71. Faarvang, H. J. (1965) *Scand. J. Clin. Lab. Invest.* **17,** 1–78
72. Kida, D., Yoneda, M., Miyaura, S., Ishimaru, T., Yoshida, Y., Ito, T., Ishiguro, N., Iwata, H., and Kimata, K. (1999) *J. Rheumatol.* **26,** 1230–1238
73. Yingsung, W., Zhuo, L., Morgelin, M., Yoneda, M., Kida, T., Watanabe, H., Ishiguro, N., Iwata, H., and Kimata, K. (2003) *J. Biol. Chem.* **278,** 32710–32718
74. De La Motte, C. A., Hascall, V. C., Drazba, J., Bandyopadhyay, S. K., and Strong, S. A. (2003) *Am. J. Pathol.* **163,** 121–133
75. Laurent, T. C. (1987) *Acta Otolaryngol. Suppl.* **442,** 7–24
76. Laurent, T. C. (1998) in *The Chemistry, Biology and Medical Applications of Hyaluronan and Its Derivatives* (Laurent, T. C., ed) pp. 305–314, Portland Press, London
77. Olsen, E. H., Rahbek-Nielsen, H., Thogersen, I. B., Roepstorff, P., and Enghild, J. J. (1998) *Biochemistry* **37,** 408–416

Materials Transactions, Vol. 45, No. 4 (2004) pp. 989 to 993
Special Issue on Frontiers of Smart Biomaterials

Bonelike Apatite Coating on Skeleton of Poly(lactic acid) Composite Sponge

Hirotaka Maeda*[1], Toshihiro Kasuga*[2] and Masayuki Nogami

Graduate School of Engineering, Nagoya Institute of Technology, Nagoya 466-8555, Japan

A novel sponge, coated with bonelike apatite (b-HA) on its skeleton surface, was prepared using a particle-leaching technique combined with a biomimetic processing. A powder mixture consisting of calcium carbonate/poly(lactic acid) composite (CCPC) and sucrose was hot-pressed and then the resulting compact was soaked in the simulated body fluid at 37°C. Within the first hour, the sucrose was completely dissolved out, resulting in the formation of large-sized pores in the compact, and subsequently, after 3 hours of soaking, b-HA formed on the skeleton consisting of CCPC. On the other hand, on a pore-free CCPC, the apatite started to form after 12~18 hours. The induction period for b-HA formation on the skeleton of the CCPC sponge prepared using a particle-leaching technique is significantly shorter than that of the pore-free CCPC. The short period is suggested to originate from that a large amount of Ca^{2+} ion is rapidly supplied into the compartment space (pore) from the CCPC skeleton. The formed sponge has numerous, large pores of 450~580 μm in diameter, which are connected with channels having a diameter in the range of 70~120 μm, as well as a high porosity of 75%. Animal test using rats showed that the sponge has osteoconduction. The sponge is expected to be one of the promising candidates for osteoconducting fillers or tissue-engineering scaffolds.

(Received October 20, 2003; Accepted December 19, 2003)

Keywords: *bonelike apatite, sponge, poly(lactic acid), calcium carbonate, simulated body fluid, osteoconduction*

1. Introduction

Engineering living tissue for reconstructive surgery requires an appropriate cell source, optimal culture conditions, and a biodegradable scaffold as the basic elements. A scaffolding material is used either to induce formation of bone from the surrounding tissue or to act as a carrier or template for implanted bone cells or other agents. To serve as a scaffold, the material must be biocompatible, osteoconductive, and have a macroporous structure. Calcium phosphate ceramics such as hydroxyapatite or tricalcium phosphate, which have a osteoconductivity, were reported to be applied to scaffolds for bone tissue engineering.[1-3]

Recently, much attention has been paid to bonelike hydroxycarbonate apatite (b-HA) as a novel biomaterial, since b-HA is very similar to the apatite in terms of living bone in its chemical composition and structure[4] and shows effective compatibility in cell attachment, proliferation, and differentiation on the material,[5] *i.e.*, osteoconductivity, as well as good bioresorbability.[6] We expect that the sponges composed of b-HA skeleton can be applied to bone-fillers or scaffolds for tissue engineering. However, in general, ceramics have brittleness and low resistance against an impact loading. Such ceramic sponge materials have a serious risk to be broken in normal handling during operations. To eliminate this risk, it has been reported that the composites were fabricated using the polymer sponge coated with bioactive materials such as hydroxyapatite or Bioglass.[7-9]

We reported earlier that a compact of calcium carbonate (vaterite)/poly(lactic acid) composite (CCPC) was reported to form b-HA on its surface even after 3 hours of soaking in SBF at 37°C.[10] The rapid formation of the b-HA was suggested to originate from the integration of PLA having carboxy groups bonded with Ca^{2+} ions for b-HA nucleation and a large amount of calcium carbonate (vaterite) having an ability to effectively increase the supersaturation of b-HA due to the fast dissolution of the nano-sized vaterite. We believe that various novel biomaterials can be prepared using CCPC.

In the present work we biomimetically prepared the novel sponge composed of PLA composite skeleton coated with b-HA utilizing CCPC for applications to osteoconducting, bioresorbable bone-fillers or tissue engineering scaffolds.

2. Experimental Procedure

We have already reported that the CCPC containing ~30% calcium carbonate has an excellent mechanical properties with a high HCA-forming ability in SBF.[11] The composite containing 30% calcium carbonate shows bending strength of 40~55 MPa, Young's modulus of 3.5~6 GPa, and significant ductility. In the present work the weight ratio of $CaCO_3$/PLA was determined to be 1/2.

Calcium carbonates consisting of vaterite were prepared by a carbonation process in methanol.[12] CO_2 gas was blown for 3 hours at a flow rate of 300 mL/min into the suspension consisting of 7.0 g of $Ca(OH)_2$ in 180 mL of methanol at 0°C in a Pyrex® beaker. The resultant slurry was dried at 70°C in air, resulting in fine-sized powders. 2.0 g of PLA (with a molecular weight of 160 ± 20 kDa, determined by gel permeation chromatography) was dissolved in 20 mL of methylene chloride at room temperature. The calcium carbonate powders were added to the PLA solution and then the mixture was stirred to prepare a PLA slurry including the calcium carbonate powders.

The sponge was prepared using a conventional particle-leaching technique. In the present work sucrose was used as a sacrificial phase. Sucrose particles, which were sieved with the opening from 0.5~1.0 mm, were added to the PLA slurry. The nominal weight ratio of CCPC/sucrose was 1/6. The slurry mixture was stirred and then cast into a stainless steel die, and subsequently dried in air for solidification. After that, the product in the die was heated at 180°C and uniaxially hot-pressed at the temperature under a pressure of 40 MPa to

*[1]Graduate Student, Nagoya Institute of Technology
*[2]Corresponding author, E-mail: kasuga.toshihiro@nitech.ac.jp

prepare a CCPC/sucrose composite (denoted by sample A). After the hot-pressing, the specimen was cut in methanol with a diamond saw.

The hot-pressed sample was soaked in SBF (consisting of 2.5 mM of Ca^{2+}, 142.0 mM of Na^{+}, 1.5 mM of Mg^{2+}, 5.0 mM of K^{+}, 148.8 mM of Cl^{-}, 4.2 mM of HCO_3^{-}, 1.0 mM of HPO_4^{2-}, and 0.5 mM of SO_4^{2-}) that included 50 mM of $(CH_2OH)_3CNH_2$ and 45.0 mM of HCl at pH 7.4 at 37°C. After soaking, the sample was removed from SBF, gently washed with distilled water, and dried at room temperature. Our strategy for the preparation of the sponge composed of CCPC skeleton coated with b-HA is to leach out the sucrose phase and simultaneously to form b-HA on the composite skeleton.

The crystalline phases in the sponge were identified by X-ray diffraction analysis (XRD). The morphology of the sponge was observed by scanning electron microscopy (SEM). The pore size distribution of the sponge was measured by mercury porosimetry. The compressive strength of the sponge (7 mm × 7 mm × 10 mm) prepared by soaking in SBF for 3 days was estimated by a compressing test at a loading rate of 1 mm/min. Concentrations of Ca^{2+} and P^{5+} ions after soaking sample (10 mm × 10 mm × 5 mm) in SBF were determined by inductively coupled plasma atomic emission spectroscopy (ICP-AES). A compact of CCPC containing no sucrose powders (denoted by sample B), with the composition of $CaCO_3$/PLA = 1/2 in weight ratio, was used as a control material to compare with sample A (sponge).

The sponge (2-mm diameter × 10-mm thickness) prepared by soaking in SBF for 3 days was implanted into a femur of a 12-week-old Wister rat (male, weight; 265~285 g). The sponge was harvested and used for histological analysis at 4 weeks after implantation. The specimen was fixed, decalcified, embedded in paraffin, and stained with hematoxylin and eosin (HE). The specimen was observed with optical microscope.

3. Results & Discussion

Figure 1 shows XRD patterns before and after soaking the compact of CCPC/sucrose mixture in SBF. The XRD pattern before soaking shows that the hot-pressed compact consists of crystalline phases such as PLA, vaterite, aragonite and sucrose. After 1 hour of soaking, the peaks corresponding to sucrose and vaterite disappear; those to PLA and aragonite are seen. Sucrose was found to be completely dissolved even after 1 hour of soaking, resulting in formation of a sponge consisting of PLA and aragonite crystals. After 1 day of soaking, an additional broad peak at around $2\theta \sim 32°$, due to b-HA, is seen with the peaks due to PLA and aragonite.

Figure 2 shows the SEM photographs of the sample after 3 days of soaking in SBF. The SEM photograph shows that the sponge has numerous, large pores of 450~580 μm in diameter and large interconnected channels of 70~120 μm. The sponge has continuous open foams with a 3D interpenetrating network of struts and pores. As shown in Fig. 2(b), the surface of the CCPC skeleton is covered with the numerous deposits, that is b-HA, judged from the XRD pattern and the morphology. Further experiments showed

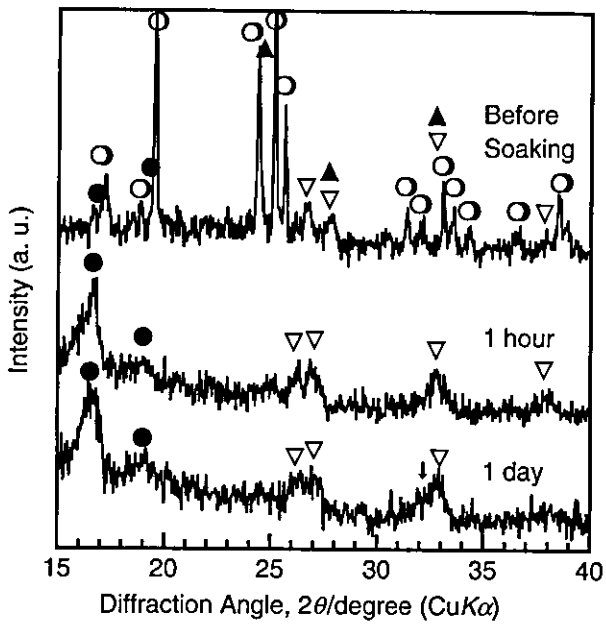

Fig. 1 XRD patterns of before and after soaking the compact of CCPC/sucrose mixture in SBF. (○) sucrose, (▲) vaterite, (▽) aragonite, (●) PLA, and (↓) apatite.

that apatite formation starts to occur after 3 hours of soaking.

Figure 3 shows the pore size distribution of the sponge prepared by soaking in SBF for 3 days. The median pore size of the sponge is 125 μm. There exist almost no pores below several tens micrometers in diameter. When a compact of the powder-mixture consisting of CCPC and sucrose was hot-pressed at 180°C, the sucrose particles melted (it begins to melt at 160°C), leading to adjacent particles connected each other. As a result, both the sucrose and CCPC phases were unified into an interconnecting three-dimensional network. The porosity was estimated from the measurement to be ~75%. The macroporous structure of the sponge prepared using sucrose may be likely to allow the migration of cells into the interior of the sponge. On the other hand, for comparison, when the sponge was prepared using sodium chloride, which were sieved with the opening from 0.5 to 1.0 mm, the median pore size in the sponge was estimated to be 65 μm. There exist numerous pores several tens micrometers in diameter. Since no sodium chloride melts during hot-pressed at 180°C, large-sized, interconnected particles as the sacrificial phase would not form.

In order to investigate apatite formation on CCPC in SBF after dissolution of the sucrose particles, the thicknesses of b-HA particles formed in SBF on the skeleton of sample A (the sponge derived from the compact of CCPC/sucrose mixture) and sample B were measured from cross-sectional SEM observation of their fracture face. The skeleton surface of sample A (sponge) was covered with numerous b-HA deposits after 3 hours of soaking (Fig. 2(b)). The b-HA formation did not occur within 2 hours. On the other hand, the surface of sample B was completely covered with b-HA after 18 hours of soaking. No b-HA formed on sample B within 12 hours. Figure 4 shows the thicknesses of b-HA layers formed on the skeleton surface of sample A or the surface of sample B as a function of the soaking time in SBF. The thickness of

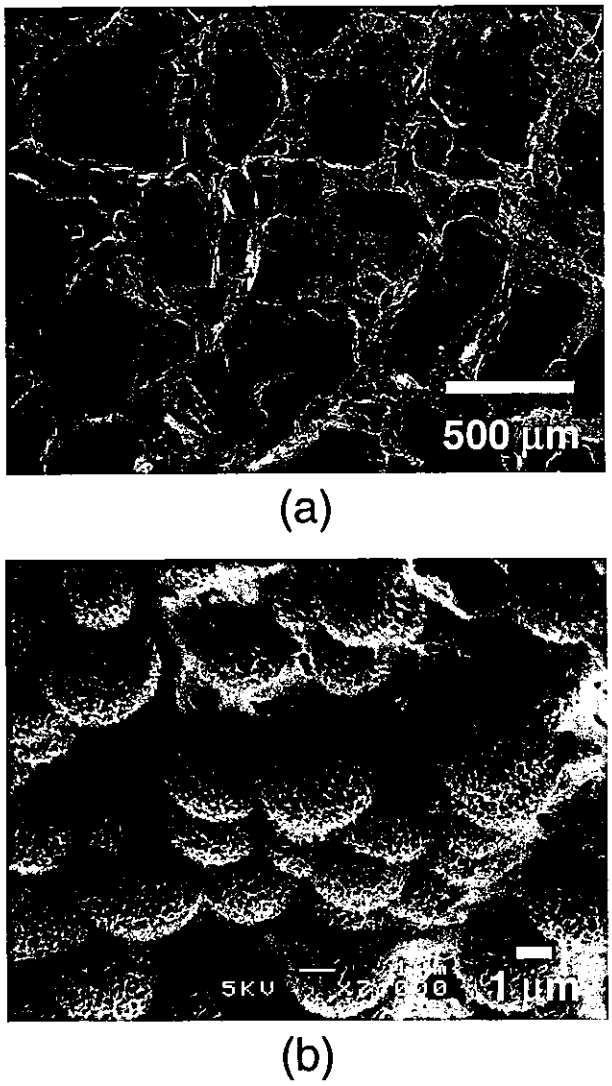

Fig. 2 SEM photographs of the sponge prepared by soaking in SBF for 3 hours. (a) cut surface of the sponge and (b) the magnified image of the skeleton surface.

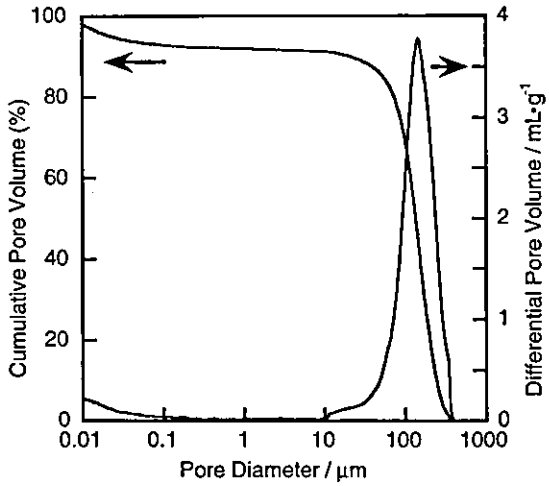

Fig. 3 Pore size distribution of the sponge prepared by soaking in SBF for 3 days.

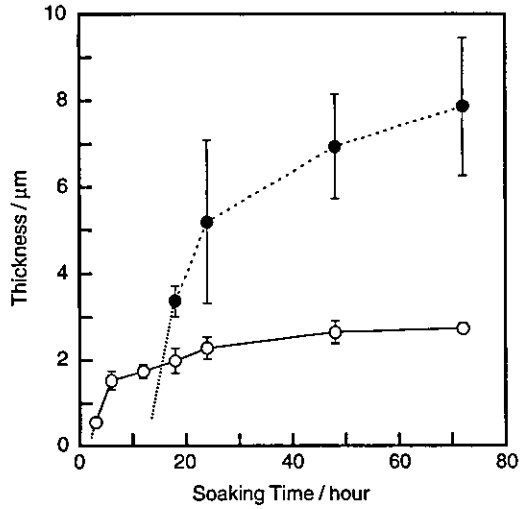

Fig. 4 Relationship between thickness of b-HA layer and soaking time in SBF. (○) sample A (the sponge) and (●) sample B.

b-HA particles on these substrates was measured using at least five points in SEM micrographs of their fracture faces and the mean thickness of b-HA particles and the standard deviation were shown. The induction period for b-HA formation on sample A is shorter than that of sample B. However, the crystal growth rate on sample B is higher than that on sample A.

When the sample A is soaked in SBF, the surface area of CCPC increases after the rapid dissolution of sucrose particles. This is suggested to be increased in the adsorption amount of Ca^{2+} and P^{5+} ions in SBF on the sponge skeleton. Figure 5 shows the amount of Ca^{2+} and P^{5+} ions after soaking sample A or sample B in SBF for various periods. When sample A is soaked, the Ca^{2+} ion amount in SBF increases slightly at the initial stage, and subsequently decreases gradually. It is proposed that the amount of the dissoluble vaterite particles, which come into contact with water, increases after dissolution of sucrose, resulting in the increase in the amount of Ca^{2+} ion released in SBF. On the other hand, after sample B is soaked in SBF, the Ca^{2+} ion amount decreases gradually. The P^{5+} ion amount in SBF

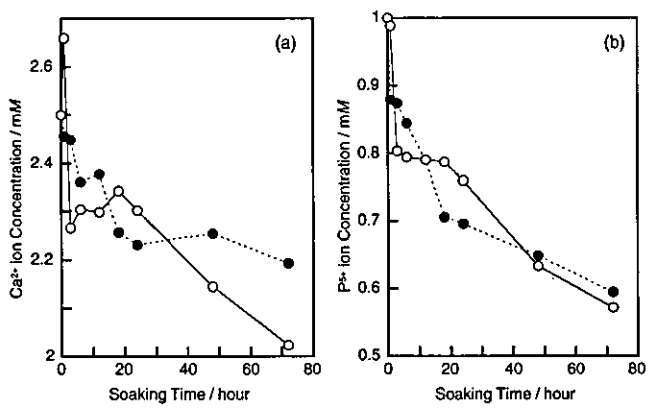

Fig. 5 Concentrations of (a) Ca^{2+} and (b) P^{5+} ions in 100 mL of SBF before and after soaking in SBF. (○) sample A (the sponge) and (●) sample B.

decreases gradually after soaking sample A or B. The phosphorous element in SBF is suggested to adsorb on CCPC as a phosphate ion.

The reduction of the induction period for b-HA formation on the CCPC sponge is suggested to be influenced by the porous structure. When the sample A is soaked in SBF, the surface area of CCPC increases due to the dissolution of the sucrose particles. As a result, a large amount of vaterite in the CCPC sponge skeleton rapidly dissolved. The pores in the sponge are considered as compartmental spaces with channels. In comparison with the surface of sample B, the supersaturation concerning b-HA around the surface of pores in the sponge (sample A) is suggested to increase rapidly. As a result, the induction period for b-HA formation on sample A is reduced. Figure 2(a) shows that the thickness of the sponge skeleton is in a range of 50~100 μm. Almost all of vaterite is dissolved within 1 hour after soaking (Fig. 1); almost no Ca^{2+} ions can be newly released from CCPC since 1 hour of soaking. As a result, the crystal growth rate on the sponge skeleton (sample A) may be suppressed. The b-HA growth rate may be also attributed to the surface area. The amount of carboxy group, which is known to induce b-HA nucleation,[13] increases with increase in surface area of the PLA portion due to the dissolution of sucrose and vaterite during the preparation of the sponge. The adsorption amount of the phosphate ion per unit surface area on the sponge skeleton may be smaller than that on the surface of sample B. As a result, the b-HA growth rate would be strictly suppressed.

Figure 6 shows a typical stress-strain curve measured by a compressive tester for the sponge prepared by soaking in SBF for 3 days. The sponge shows the compressive strength of ~1.5 MPa and the maximum strain for the fracture of the sponge is over 10%, which is two orders of magnitude larger than that of a dense hydroxyapatite ceramic.[14] The curve also shows that the fracture proceeds gradually beyond the maximum stress; the sponge leads to ductile fracture. The sponges in the present work are not broken in normal handling during operations.

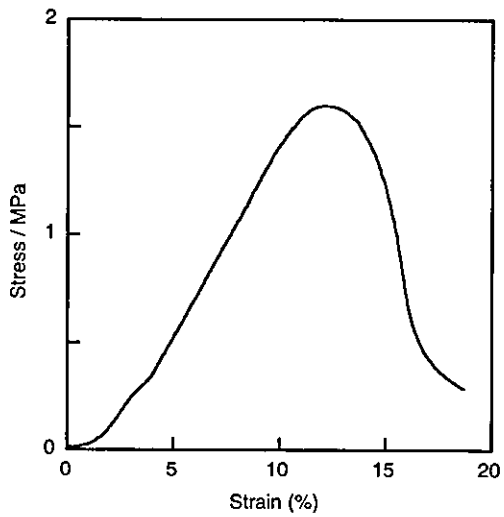

Fig. 6 Typical stress-strain curve in a compressive test of the sponge prepared by soaking in SBF for 3 days.

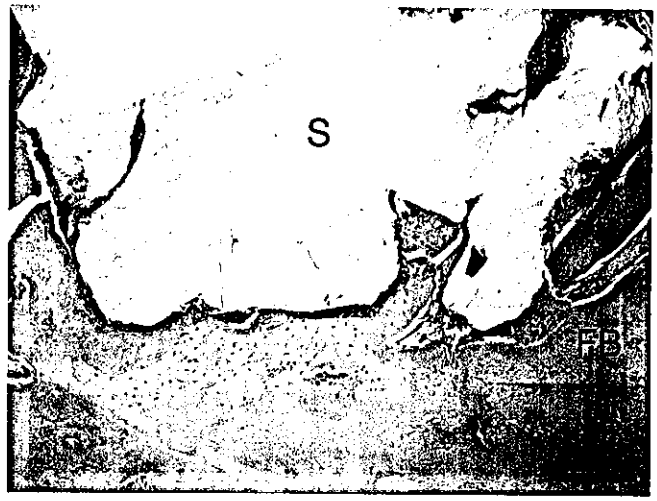

Fig. 7 The optical micrograph of a decalcified section of the sponge after implantation into a femur of a rat for 4 weeks. (S) the sponge, (NB) native bone, and (FB) newly formed bone. The section was stained with hematoxylin and eosin. Bar scale is 100 μm.

Figure 7 shows the decalcified sections stained with HE at 4 weeks postimplantation; newly bone formed in the pore. This figure shows that newly formed bone continues to be present in direct contact with the sponge without intervening soft tissues. No adverse tissue response and inflammation reaction were seen around the implant. The present osteoconducting sponge is also expected to have bioresorbability. Further histological investigation is in progress.

4. Conclusion

Coating with b-HA on CCPC sponge skeleton surface can be easily prepared in a short time utilizing a sucrose-particle-leaching technique combined with a biomimetic processing. The induction period for b-HA formation on the CCPC sponge skeleton is significantly shorter than that of a CCPC compact without sucrose. The sponge prepared using sucrose has numerous, large pores of 450~580 μm in diameter, which are connected with channels having a diameter in the range of 70~120 μm, as well as a high porosity of 75%. The sponge is expected to allow the migration of cells into the interior of the sponge. It is not broken in normal handling during operations. Animal test using rats showed that the present material has a osteoconductivity. The sponge is one of the great potential candidates as bone-fillers or scaffolds for tissue engineering.

Acknowledgements

The present work was supported in part by a Grant-in-Aid for Scientific Research from Japan Society for the Promotion of Science and by a grant from the NITECH 21st Century COE Program "World Ceramics Center for Environmental Harmony".

REFERENCES

1) T. Noshi, T. Yoshikawa, M. Ikeuchi, Y. Dohi, H. Ohgushi, K. Horiuchi, M. Sugimura, K. Ichijima and K. Yonemasu: J. Biomed. Mater. Res. 52

(2000) 621–630.
2) J. Dong, T. Uemura, Y. Shirasaki and T. Tateishi: Biomater. **23** (2002) 4493–4502.
3) T. Yoshikawa, H. Nakajima, E. Yamada, M. Akahane, Y. Dohi, H. Ohgushi, S. Tamai and K. Ichijima: J. Bone Miner. Res. **15** (2000) 1147–1157.
4) T. Kokubo: Acta Mater. **46** (1998) 2519–2527.
5) Y. Doi: Cells and Mater. **7** (1997) 111–122.
6) Y. Doi, T. Shibutani, Y. Moriwaki and Y. Iwayama: J. Biomed. Mater. Res. **39** (1998) 603–610.
7) H. R. Ramay and M. Zhang: Biomater. **24** (2003) 3293–3302.
8) R. Zhang and P. X. Ma: J. Biomed. Mater. Res. **45** (1999) 285–293.
9) J. A. Roether, A. R. Boccaccini, L. L. Hench, V. Maquet, S. Gautier and R. Jérôme: Biomater. **23** (2002) 3871–3878.
10) H. Maeda, T. Kasuga, M. Nogami, Y. Hibino, K. Hata, M. Ueda and Y. Ota: J. Mater. Res. **17** (2002) 727–730.
11) T. Kasuga, H. Maeda, K. Kato, M. Nogami, K. Hata and M. Ueda: Biomater. **24** (2003) 3247–3253.
12) K. Nakamae, S. Nishiyama, J. Yamashiro, Y. Fujimura, A. Urano and Y. Tosaki: Nihon-Setchaku-Kyokai-shi (in Japanese) **21** (1985) 414–450.
13) M. Tanahashi and T. Matsuda: J. Biomed. Mater. Res. **34** (1997) 305–315.
14) H. Aoki: *Mechanical Properties*, (Medical Application of Hydroxyapatite, Tokyo, 1994) pp. 286–306.

ELSEVIER

Science and Technology of Advanced Materials 6 (2005) 48-53

SCIENCE AND TECHNOLOGY OF ADVANCED MATERIALS

www.elsevier.com/locate/stam

Preparation of bonelike apatite composite for tissue engineering scaffold

Hirotaka Maeda[a], Toshihiro Kasuga[a,*], Masayuki Nogami[a], Minoru Ueda[b]

[a]*Department of Materials Science and Engineering, Graduate School of Engineering, Nagoya Institute of Technology, Gokiso-cho, Showa-ku, Nagoya 466-8555, Japan*

[b]*Nagoya University Graduate School of Medicine, Tsurumai-cho 65, Showa-ku, Nagoya 466-8550, Japan*

Received 8 March 2004; revised 7 June 2004; accepted 15 July 2004

Abstract

A novel sponge composed of a poly (lactic acid) composite skeleton covered with bonelike apatite (b-HA) was produced via a particle-leaching technique combined with a biomimetic processing. The sponge has a large porosity of ~75% with large-sized pores and shows mechanical ductility. After incubation of human osteoblasts for 7 days, numerous cells attached to the surface of the skeleton, which was covered with b-HA. One result of the osteoclastic cell culture showed that the b-HA on the composite has excellent bioresorbability. The sponge is expected to be one of the promising candidates for bone tissue engineering scaffolds.

Keywords: Bonelike apatite; Sponge; Poly(lactic acid); Vaterite; Simulated body fluid; Cell-compatibility

1. Introduction

While historically, organic tissue has been employed in the repair of bone defects; more recently, attention has been paid to synthetics, which may obviate the problems arising from the use of organic tissue in bone grafting. The use of all allografts carries the risk of disease transmission and tissue rejection, while autografts present problems of limited supply and donor site morbidity. These facts have made synthetic grafts an alternative to organic grafts. Some ceramics, such as Bioglass®, sintered hydroxyapatite and glass–ceramic A–W, have been shown to spontaneously bond to living bone [1–3]. They are called bioactive materials, and are already in clinical use as important bone-repairing materials. These materials could promote the generation of new bone by acting as a scaffold for osseous growth, but they are only osteoconductive and not osteoinductive.

Vacanti et al. have developed a new technique called 'tissue engineering' [4]. Engineering living tissue for reconstructive surgery requires an appropriate cell source, optimal culture conditions, and a biodegradable scaffold as the basic elements. A scaffolding material is used either to induce formation of bone from the surrounding tissue or to act as a carrier or template for implanted bone cells or other agents. To serve as a scaffold for bone tissue engineering, the material must be biocompatible, osteoconductive, and have a macroporous structure. Calcium phosphate ceramics such as hydroxyapatite or β-tricalcium phosphate (β-TCP), which have osteoconductivity, were reported to have been applied to scaffolds for bone tissue engineering [5,6].

Recently, much attention has been paid to bonelike hydroxycarbonate apatite (b-HA) as a novel biomaterial, since b-HA is very similar to apatite in terms of living bone in its chemical composition and structure [7] and shows effective compatibility in cell attachment, proliferation, and differentiation on the material [8], as well as good bioresorbability [9]. We expect that the sponges composed of b-HA skeleton can be applied to scaffolds for bone tissue engineering. In general, ceramics show brittleness and low resistance against impact loading. Such ceramic sponge materials have a serious risk of breaking in normal handling during operations. To eliminate this risk, it has been reported that the composites were fabricated using a polymer sponge coated with bioactive materials such as hydroxyapatite or Bioglass® [10,11].

* Corresponding author. Tel./fax: +81 52 735 5288.
E-mail address: kasuga.toshihiro@nitech.ac.jp (T. Kasuga).

1468-6996/$ - see front matter © 2005 Published by Elsevier Ltd.
doi:10.1016/j.stam.2004.07.003

A preparation method for b-HA using simulated body fluid (SBF), which is a tris-buffer solution with inorganic ion concentrations almost equal to those of human plasma, is called a biomimetic method [12]. This method has an advantage over conventional methods in that materials can be coated with b-HA without heating. Two indispensable conditions needed for the formation of b-HA on materials using SBF are (1) the existance of the surface functional groups that induce nucleation of b-HA and (2) increase in the supersaturation of b-HA in SBF [3,13,14].

Poly(lactic acid) (PLA) with many carboxy groups is one of the promising candidates for supplying inducers for the b-HA nucleation. A carboxy group, which is known to induce b-HA nucleation [13], can be formed by the hydrolyzation of PLA. To increase the supersaturation of b-HA in SBF, a large amount of Ca^{2+} ions should be dissolved from the materials. Bioresorbable calcium carbonate is expected to provide Ca^{2+} ions for SBF resulting in an increase in the supersaturation of b-HA. It is well known that calcium carbonate has three polymorphs, viz. calcite, aragonite and vaterite. The solubility of vaterite is higher than that of calcite or aragonite [15]. We have already reported that the PLA composites containing vaterite have much higher b-HA-forming ability in SBF than the composites containing calcite or aragonite without vaterite [16]. In our earlier work a pellet of a powder mixture consisting of 25 wt% biodegradable PLA and 75 wt% nano-sized calcium carbonate (vaterite) was reported to form b-HA on its surface even after being soaked for 3 h in SBF [17]. It was suggested that rapid formation of the b-HA originated from the fact that PLA contains carboxy groups that are bonded with Ca^{2+} ions for the b-HA nucleation, and a large amount of vaterite, which has the ability to effectively increase the supersaturation of the b-HA. We believe that various novel biomaterials can be prepared using PLA and vaterite. Hereafter, the composites are denoted by CCPC (Calcium Carbonate/Poly(lactic acid) Composites).

In the present work, we biomimetically prepared a novel sponge composed of PLA composite skeleton covered with b-HA utilizing CCPC. The present study also involves the evaluation of cell-compatibility on CCPC covered with b-HA for application to tissue engineering scaffolds.

2. Experimental method

2.1. Preparation of vaterite powders

Vaterite was prepared by a carbonation process using methanol [18]. CO_2 gas was blown for 3 h at a flow rate of 300 mL/min into the suspension consisting of 7.0 g of $Ca(OH)_2$ in 180 mL of methanol at 0 °C in a Pyrex® beaker. The resultant slurry was dried at 70 °C in air, resulting in fine-sized powders. Fig. 1 shows an X-ray diffraction (XRD) pattern and scanning electron microscopy (SEM) photograph of the vaterite powders. The XRD pattern shows that the calcium carbonate powders obtained in the present work consist predominantly of vaterite with small amounts of aragonite and calcite. The SEM photograph shows that secondary particles of $\leq$500 nm diameter were formed as an agglomeration of primary particles of $\sim$100 nm. The BET surface area was measured to be $\sim$40 m^2/g.

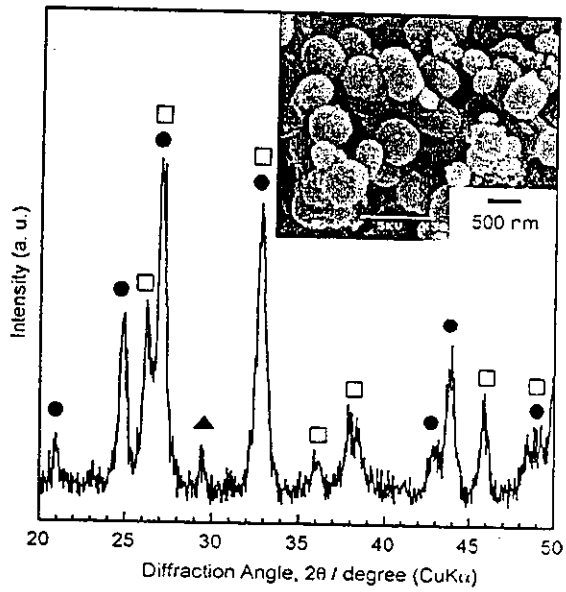

Fig. 1. The XRD pattern of vaterite powders prepared by a carbonation process in methanol. (●) vaterite, (▲) calcite, and (□) aragonite. Inset shows the SEM photograph of vaterite.

2.2. Preparation of PLA composites containing vaterite powders

PLA produced by Shimadzu Corp. (LACTY#2012) was used as a matrix phase. PLA with a molecular weight of 160±20 kDa, determined by gel permeation chromatography, was dissolved in methylene chloride at room temperature. The vaterite powders were added to the PLA solution and the mixture was then stirred. The weight ratio of vaterite/PLA was 1/2. We have already reported that CCPC containing $\sim$30% vaterite has excellent mechanical properties, such as a bending strength of $\sim$50 MPa, Young's modulus of $\sim$5 GPa and ductility, with a high b-HA-forming ability in SBF [19]. The slurry mixture was stirred and cast into a stainless steel die, and then dried in air for solidification. After that, the product in the die was heated at 180 °C and uniaxially hot-pressed under a pressure of 40 MPa. After the heating, the specimen in the die was cooled to room temperature.

Fig. 2(a) shows a photo of CCPC in the present work. The sample was picked up and bent with two fingers. CCPC has high flexibility and can be cut using scissors, as shown in Fig. 2(b).

(a)

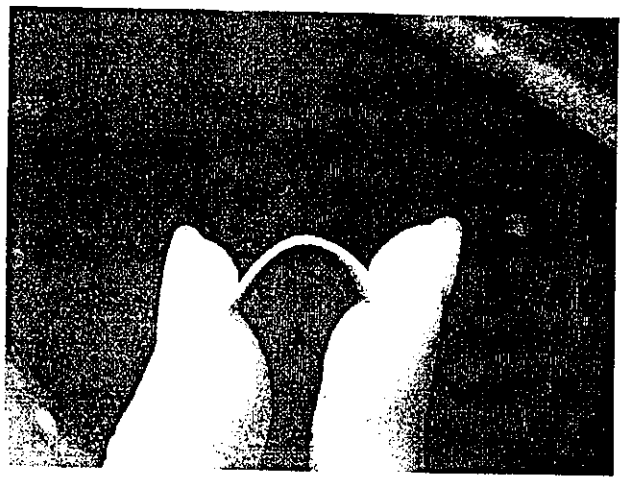

(b)

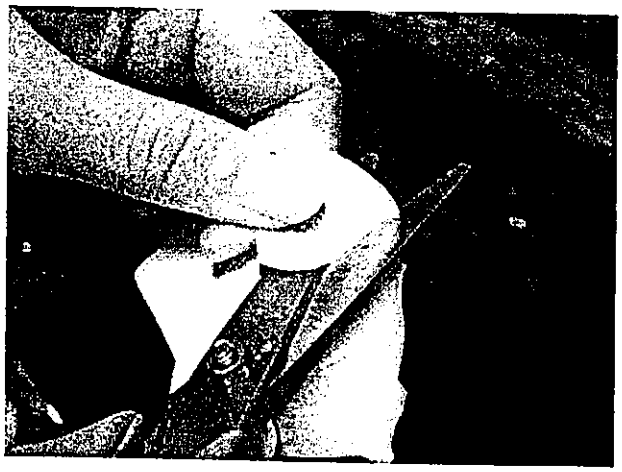

Fig. 2. Photos of (a) flexiblility test and (b) cutting test of CCPC.

2.3. Preparation of the CCPC sponge skeleton covered with b-HA

2.0 g of PLA was dissolved in 20 mL of methylene chloride at room temperature The vaterite powders were added to the PLA solution and the mixture was then stirred to prepare a PLA slurry including the vaterite powders. The weight ratio of vaterite/PLA was 1/2. The sponge was prepared using a conventional particle-leaching technique. In the present work sucrose was used as a sacrificial phase. Sucrose particles, which were sieved with an opening of from 0.5 to 1.0 mm, were added to the PLA slurry. The weight ratio of CCPC/sucrose was 1/6. The slurry mixture was stirred, cast into a stainless steel die, and subsequently dried in air for solidification. After that, the product in the die was heated at 180 °C and uniaxially hot-pressed at this temperature under a pressure of 40 MPa to prepare a CCPC/sucrose composite. After the hot-pressing, the specimen was cut in methanol with a diamond saw. Our strategy for the preparation of the sponge composed of CCPC skeleton coated with b-HA is to leach out the sucrose phase and to simultaneously form b-HA on the composite skeleton utilizing SBF (consisting of 2.5 mM of Ca^{2+}, 142.0 mM of Na^{+}, 1.5 mM of Mg^{2+}, 5.0 mM of K^{+}, 148.8 mM of Cl^{-}, 4.2 mM of HCO_3^{-}, 1.0 mM of HPO_4^{2-}, and 0.5 mM of SO_4^{2-}) that included 50 mM of $(CH_2OH)_3CNH_2$ and 45.0 mM of HCl at pH 7.4 at 37 °C as a solvent. The CCPC/sucrose composite was soaked in SBF for 3 days.

The crystalline phases in the sponge were identified by XRD, and the morphology of the sponge observed by SEM. The pore size distribution of the sponge was measured by mercury porosimetry. The compressive strength of the sponge (7×7×10 mm) was estimated by a compressing test at a loading rate of 1 mm/min.

2.4. Osteoblastic and osteoclastic cell cultures

Human bone marrow stromal cells, obtained by aspiration from the femoral diaphysis of patients were used for this experiment. The cell suspension was cultured in mesenchyaml stem cell basal medium (MSCBM, Camblex) with 10% fetal bovine serum (FBS) supplemented with 20 μg/mL L-glutamine, 1 μg/mL penicillin/streptomycine and incubated at 37 °C in a humidified atmosphere of 95% air and 5% CO_2. Two millilitres of a cell suspension containing (1×10^4 cell/mL) was plated on the CCPC sponge skeleton covered with b-HA (5×5×5 mm) and the sponge then incubated at 37 °C in 5% CO_2 for 1 week.

Osteoclasts were obtained from the long bones of 1-day-old neonatal rabbits (Japan white), following a reference [20]. A α-modified minimum essential medium (α-MEM, Gibco) supplemented with 15% FBS and antibiotics was used as the plating medium. A cell suspension (100 μL) containing 50–100 multinucleated osteoclasts/100 μL was plated onto disk shaped CCPC (with the composition of $CaCO_3$/PLA = 1/2 in weight ratio) covered with b-HA prepared by soaking in SBF for 2 days (8 mmØ × 1 mm) plated in the small wells of microculture plates. A compact of CCPC (with the composition of $CaCO_3$/PLA = 1/2 in weight ratio) was used as a control material to compare with CCPC covered with b-HA. After incubation at 37 °C in 5% CO_2 for 90 min, the unattached cells were gently washed off and the substrates were transferred into 35 mm culture medium and then incubated at 37 °C in 5% CO_2 for 2 days.

After the culturing period, the samples were fixed with glutaraldehyde in a cacodylate buffer. The cells, after being rinsed several times in the same buffer, were post-fixed in 1% osmium tetraoxide and dehydrated through graded ethanols. The samples were freeze-dried with *tert*-butyl alcohol and coated with osmium. The morphology of osteoblasts and osteoclasts, and the resorption lacunae produced by osteoclasts on the surface of the substrates were observed with SEM.

3. Results and discussion

3.1. CCPC sponge skeleton covered with b-HA

Fig. 3 shows the SEM photographs, the XRD pattern, and the pore size distribution of the sample following 3 days of soaking in SBF. The SEM photograph shows that the sponge has numerous, large pores of 450–580 μm in diameter and large interconnected channels of 70–120 μm. The sponge has continuous open foams with a 3D interpenetrating network of struts and pores, while the surface of the CCPC sponge skeleton is covered with numerous deposits. In Fig. 3(b), it is clear that, although an XRD peak of $2\theta \sim 32°$ resulting from the HA is not clear due to superimposition on the calcium carbonate (aragonite), the peak appears anew following the treatment (in comparison with the XRD pattern of the calcium carbonates in Fig. 1). That is, judged from the XRD pattern and the morphology, the deposits are concluded to be b-HA. The pore-size distribution measured using a mercury porosimeter showed that there exist almost no pores below several tens of micrometers in diameter and the median pore size of the sponge is 125 μm. The porosity was estimated from the measurement to be ~75%. When a compact of the powder-mixture consisting of CCPC and sucrose was hot-pressed at 180 °C, the sucrose particles melted (it begins to melt at 160 °C), leading to adjacent particles connecting to each other. As a result, both the sucrose and CCPC phases were unified into an interconnecting three-dimensional network. The macroporous structure of the sponge may allow the migration of cells into the interior of the sponge.

Fig. 4 shows typical stress–strain curves measured by a compressive tester for the CCPC sponge and β-TCP sponge with the same porosity of 75%. The CCPC sponge shows the compressive strength of ~1.5 MPa and the maximum strain for the fracture of the sponge is over 10%. The curve of the CCPC sponge also shows that the fracture proceeds gradually beyond the maximum stress; the sponge leads to ductile fracture. On the other hand, although the β-TCP sponge has strength close to that of the CCPC sponge, the stress–strain curve shows a typically brittle fracture. The CCPC sponge in the present work will not break in normal handling during operations. This ductility is believed to be an important mechanical property for the tissue engineering.

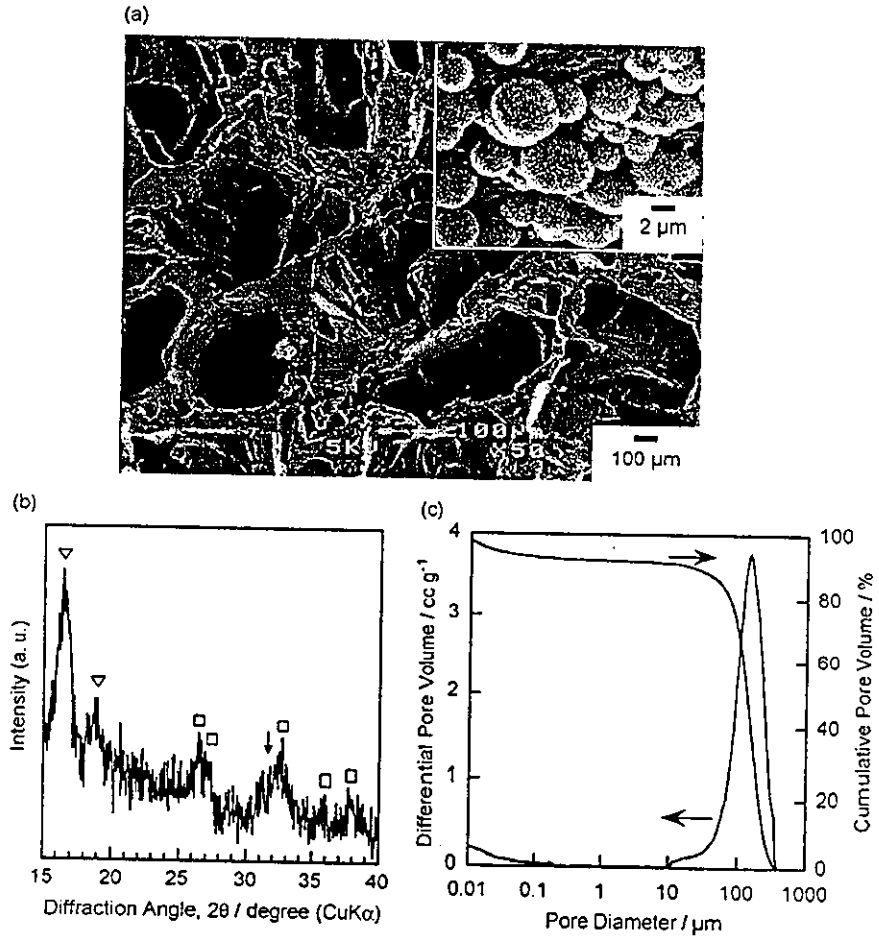

Fig. 3. (a) SEM photographs of the cut surface, (b) the XRD pattern, and (c) the pore size distribution of the sponge prepared in the present work.. (□) aragonite, (▽) PLA, and (↓) apatite. Inset shows the magnified image of the skeleton surface.

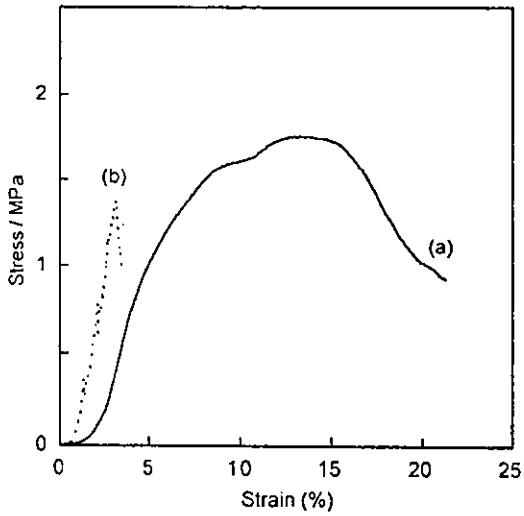

Fig. 4. Typical stress–strain curves of (a) the CCPC sponge and (b) β-TCP sponge in a compressive test.

3.2. Cells culture on CCPC

Fig. 5 shows a cross-sectional SEM photograph of the skeleton surface around the center of the CCPC sponge following one-week incubation. Numerous cells were attached to the skeleton covered with b-HA. We believe that cells can migrate through the channels into the interior of the sponge. SEM observation showed that the adhesion of cells on the skeleton covered with b-HA is larger than that on the sponge skeleton composed of PLA. This suggests that the presence of the b-HA layer on CCPC induces an effective increase in the attachment of the cells.

Fig. 6 shows SEM photographs of the osteoclast on the surface of CCPC covered with b-HA and CCPC after incubation for 2 days. The resorption lacuna was evident on the surface of these substrates. This area was widespread with a diameter of more than 25 μm on CCPC covered with b-HA. The attacks (~15 μm of diameter) on CCPC are

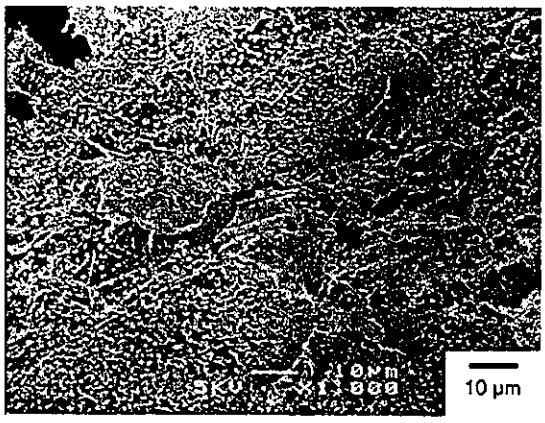

Fig. 5. The SEM photograph of the skeleton surface covered with b-HA around the center of the CCPC sponge after incubation of osteoblastic cells for one week.

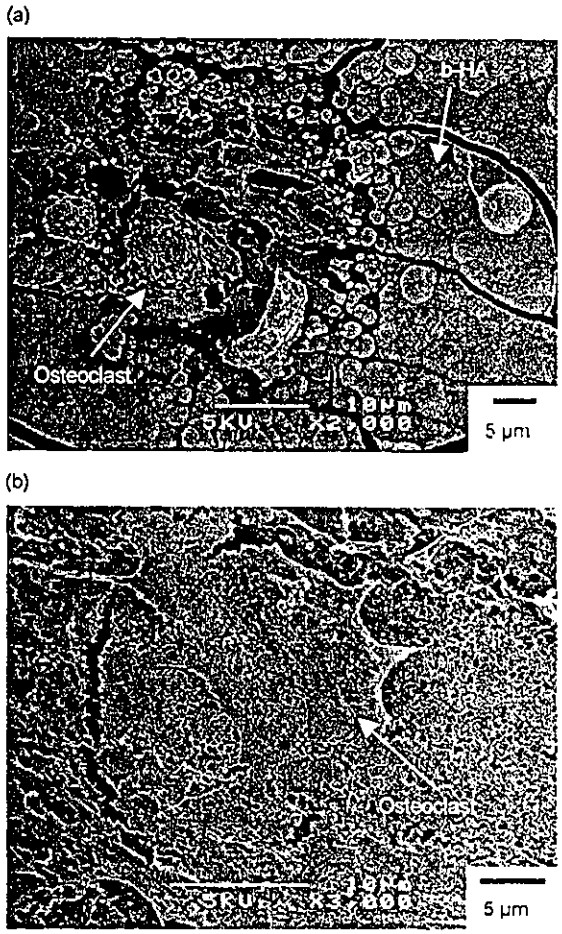

Fig. 6. The SEM photograph of the surface of (a) the CCPC covered with b HA and (b) CCPC after incubation of osteoclastic cells for 2 days.

smaller than that on CCPC with b-HA. Although further statistical analysis concerning the difference between the lacuna sizes of the samples is needed, Fig. 6 clearly shows the different bioresorption behaviors; the b-HA layer on the CCPC increases the resorption produced by osteoclasts.

4. Conclusion

A novel sponge, covered with b-HA on its skeleton surface, was prepared using a particle-leaching technique combined with a biomimetic processing. The formed sponge has numerous, large pores of 450–580 μm in diameter, which are connected with channels having a diameter in the range of 70–120 μm, as well as a high porosity of 75%. The sponge is expected to allow the migration of cells into its interior, and is not broken in normal handling during operations. Cell-compatibility of the CCPC is greatly enhanced after induction of the formation of the b-HA layer. The sponge is one of the great potential candidates as scaffolds for bone tissue engineering.

Acknowledgements

The authors are indebted to Prof Yutaka Doi of Asahi University for his helpful discussion on osteoclastic culture. The present work was supported in part by a Grant-in-Aid for Scientific Research from the Japan Society for the Promotion of Science and by a grant from the NITECH 21st Century COE Program 'World Ceramics Center for Environmental Harmony'.

References

[1] L.L. Hench, Bioceramics: from concept to clinic, Journal of American Ceramic Society 74 (1991) 1487–1510.
[2] M. Jarcho, J.F. Kay, K.I. Gumaer, R.H. Doremus, H.P. Drobeck, Tissue, cellular and subcellular events at a bone-ceramic hydroxylapatite interface, Journal of Bioengineering 1 (1977) 79–92.
[3] T. Kokubo, Surface chemistry of bioactive glass–ceramics, Journal of Non-Crystalline Solids 120 (1990) 138–151.
[4] C.A. Vacanti, R. Langer, B. Schloo, J.P. Vacanti, Synthetic polymer seeded with chondrocytes provide a template for new cartilage formation, Plastic and Reconstructive Surgery 88 (1991) 753–759.
[5] J. Dong, T. Uemura, Y. Shirasaki, T. Tateishi, Promotion of bone formation using highly pure porous β-TCP combined with bone marrow-derived osteoprogenitor cells, Biomaterials 23 (2002) 4493–4502.
[6] T. Noshi, T. Yoshikawa, M. Ikeuchi, Y. Dohi, H. Ohgushi, K. Horiuchi, M. Sugimura, K. Ichijima, K. Yonemasu, Enhancement of the in vivo osteogenic potential of marrow/hudroxyapatite composites by bovine bone morphogenetic protein, Journal of Biomedical Materials Research 52 (2000) 621–630.
[7] M. Neo, T. Nakamura, C. Ohtsuki, T. Kokubo, T. Yamamuro, Apatite formation on three kinds of bioactive material at an early stage in vivo: a comparative study by transmission electron microscopy, Journal of Biomedical Materials Research 27 (1993) 999–1006.
[8] Y. Doi, Sintered carbonate apatites as bone substitutes, Cells and Materials 7 (1997) 111–122.
[9] Y. Doi, T. Shibutani, Y. Moriwaki, T. Kajimoto, Y. Iwayama, Sintered carbonate apatites as bioresorbable bone substitutes, Journal of Biomedical Materials Research 39 (1998) 603–610.
[10] R. Zhang, P.X. Ma, Porous poly(L-lactic acid)/apatite composites created by biomimetic process, Journal of Biomedical Materials Research 45 (1999) 285–293.
[11] J.A. Roether, A.R. Boccaccini, L.L. Hench, V. Maquet, S. Gautier, R. Jérôme, Development and in vitro characterisation of novel bioresorbable and bioactive composite materials based on polylactide foams and Bioglass® for tissue engineering applications, Biomaterials 23 (2002) 3871–3878.
[12] T. Kokubo, Apatite formation on surfaces of ceramics, metals and polymers in body environment, Acta Materialia 46 (1998) 2519–2527.
[13] M. Tanahashi, T. Yao, T. Kokubo, M. Minoda, T. Miyamoto, T. Nakamura, T. Yamamuro, Apatite coated on organic polymers by biomimetic process: improvement in its adhesion to substrate by NaOH treatment, Journal of Applied Biomaterials 5 (1994) 339–347.
[14] C. Ohtsuki, T. Kokubo, T. Yamamuro, Mechanism of apatite formation on calcium oxide-silica-phosphorus pentoxide glasses in a simulated body fluid, Journal of Non-Crystalline Solids 143 (1992) 84–92.
[15] T. Yasue, Y. Kojima, Y. Arai, Preparation of vaterite and control of its crystal shape, Gypsum and Lime 247 (1993) 471–480 (in Japanese).
[16] H. Maeda, T. Kasuga, M. Nogami, Y. Ota, Preparation of calcium carbonate composites and their apatite-forming ability in simulated body fluid, Journal of the Ceramics Society of Japan 2004; (in press).
[17] H. Maeda, T. Kasuga, M. Nogami, Y. Hibino, K. Hata, M. Ueda, Y. Ota, Biomimetic apatite formation on poly(lactic acid) composites containing calcium carbonates, Journal of Materials Research 17 (2002) 727–730.
[18] K. Nakamae, S. Nishiyama, J. Yamashiro, Y. Fujimura, A. Urano, Y. Tosaki, T. Matsumoto, Synthesis of calcium carbonate in methanol medium and its surface characterization, Journal of the Adhesion Society of Japan 21 (1985) 414–420 (in Japanese).
[19] T. Kasuga, H. Maeda, K. Kato, M. Nogami, K. Hata, M. Ueda, Preparation of poly(lactic acid) composites containing calcium carbonate (vaterite), Biomaterials 24 (2003) 3247–3253.
[20] T. Shibutani, N.M. Heershe, Effect of medium pH on osteoclast activity and osteoclast formation in cultures of dispersed rabbit osteoclasts, Journal of Bone and Mineral Research 8 (1993) 331–336.